JB Accepted Manuscript Posted Online 22 August 2016
J. Bacteriol. doi:10.1128/JB.00437-16

Neisseria gonorrhoeae crippled its peptidoglycan fragment permease to facilitate toxic peptidoglycan monomer release

Jia Mun Chan and Joseph P. Dillard*

University of Wisconsin-Madison
Department of Medical Microbiology and Immunology
School of Medicine and Public Health
Madison, WI 53705

Running title: Peptidoglycan recycling in *Neisseria* species

Keywords: *Neisseria gonorrhoeae*, *Neisseria meningitidis*, nonpathogenic *Neisseria*, AmpG, peptidoglycan recycling, peptidoglycan fragment release

*To whom correspondence should be addressed:
Email: jpdillard@wisc.edu
Mailing address: 1550 Linden Dr., 4157 Microbial Sciences Building, Madison WI 53706
Phone: (608) 265-2837
Fax: (608) 262-8418

ABSTRACT

Neisseria gonorrhoeae (gonococci) and *Neisseria meningitidis* (meningococci) are human pathogens that cause gonorrhea and meningococcal meningitis respectively. Both *N. gonorrhoeae* and *N. meningitidis* release a number of small peptidoglycan (PG) fragments, including proinflammatory PG monomers, although *N. meningitidis* releases less of the PG monomers. The PG fragments released by *N. gonorrhoeae* and *N. meningitidis* are generated in the periplasm during cell wall remodeling, and a majority of these fragments are transported into the cytoplasm by an inner membrane permease, AmpG; however, a portion of the PG fragments are released into the extracellular environment through unknown mechanisms. We previously reported that expression of meningococcal *ampG* in *N. gonorrhoeae* reduced PG monomer release by gonococci. This finding suggested that the efficiency of AmpG-mediated PG fragment recycling regulates the amount of PG fragments released into the extracellular milieu. We determined that three AmpG residues near the C-terminal end of the protein modulate AmpG's efficiency. We also investigated the association between PG fragment recycling and release in two species of human-associated nonpathogenic *Neisseria*, *N. sicca* and *N. mucosa*. Both *N. sicca* and *N. mucosa* release lower levels of PG fragments and are more efficient at recycling PG fragments compared to *N. gonorrhoeae*. Our results suggest that *N. gonorrhoeae* has evolved to increase the amounts of toxic PG fragments released by reducing its PG recycling efficiency.

IMPORTANCE

Neisseria gonorrhoeae and *Neisseria meningitidis* are human pathogens that cause highly inflammatory diseases, although *N. meningitidis* is also frequently found as a normal member of the nasopharyngeal microbiota. Nonpathogenic *Neisseria*, such as *N. sicca* and *N. mucosa*, also colonize the nasopharynx without causing disease. Although all four species release peptidoglycan fragments, *N. gonorrhoeae* is least efficient at recycling and releases the largest amount of proinflammatory peptidoglycan monomers, partly due to differences in the recycling permease AmpG. Studying the interplay between bacterial physiology (peptidoglycan metabolism) and pathogenesis (release of toxic monomers) leads to increased understanding of how different bacterial species maintain asymptomatic colonization or cause disease, and may contribute to efforts to mitigate disease.

INTRODUCTION

Ten species in the genus *Neisseria* are found associated with humans. *Neisseria gonorrhoeae* (gonococci, GC) and *Neisseria meningitidis* (meningococci, MC) are considered human restricted pathogens, while *N. cinerea*, *N. elongata*, *N. flavescens*, *N. lactamica*, *N. mucosa*, *N. polysaccharea*, *N. sicca*, and *N. subflava* are considered nonpathogenic. The nonpathogenic species colonize the nasopharynx and oral cavity of healthy people (1–3). In rare cases, these species disseminate to cause endocarditis or septic infection in immunocompromised individuals or trauma patients (4). *N. gonorrhoeae* and *N. meningitidis* share many infection-related factors with the nonpathogenic species including type IV pili, adhesins, and certain iron transport proteins (5). Unlike *N. gonorrhoeae* and *N. meningitidis*, nonpathogenic *Neisseria* are considered to be non-inflammatory, and very rarely elicit a symptomatic inflammatory response (6).

N. gonorrhoeae commonly infects the genitourinary tract, causing urethritis in men and cervicitis in women. In women, the bacteria can spread to the uterus and Fallopian tubes, leading to highly inflammatory conditions, endometritis, pelvic inflammatory disease, and ectopic pregnancy. Gonococci can also disseminate to cause sepsis, tenosynovitis, and meningitis (7). Disease manifestations are due to the host inflammatory response. In pelvic inflammatory disease, release of peptidoglycan (PG) fragments and endotoxin by gonococci in the Fallopian tubes induces an inflammatory response that kills the ciliated cells, and the cells come out of the epithelium and are sloughed off (8, 9). The loss of ciliated cells and the tissue damage results in tubal factor infertility or predisposes the woman to ectopic pregnancy.

N. gonorrhoeae is unusual among Gram-negative bacteria in that it releases significant amounts of PG fragments during growth (10). The most abundant fragments released are the PG monomers. These are disaccharide-tripeptide and disaccharide-tetrapeptide fragments carrying a 1,6-anhydro bond on the *N*-acetylmuramic acid residue (11). The disaccharide-tetrapeptide is identical to tracheal cytotoxin (TCT), the PG fragment released by *Bordetella pertussis* that induces death and sloughing of ciliated cells in the trachea (12–14). The disaccharide-tripeptide stimulates activation of the human pattern-recognition receptor NOD1 (15). When added to Fallopian tube tissue in organ culture, a mixture of the two monomers caused death and sloughing of ciliated cells, mimicking the tissue damage of pelvic inflammatory disease (8).

Although commonly considered a pathogen, *N. meningitidis* is a normal colonizer of the human nasopharynx and is carried asymptomatically by 10-40% of the population (16). The bacteria can spread to cause sepsis or meningitis, and approximately 550 cases of invasive meningococcal disease occur in the US every year (17). In these invasive infections, meningococci elicit a large inflammatory response that frequently results in septic shock and death of the patient within a few days of the onset of symptoms. However, *N. meningitidis* may not be inflammatory during the carriage state, only upregulating expression of virulence factors required for invasion and immune evasion under certain conditions (18).

We have investigated the mechanisms involved in the generation and release of proinflammatory PG fragments by *N. gonorrhoeae* and *N. meningitidis*. The PG monomers are generated by lytic transglycosylases, which in *Neisseria* species, are predicted outer-membrane lipoproteins (19, 20). As the bacteria grow and divide, they must degrade PG strands to make space for the incorporation of additional PG strands and remodel the cell wall to build and then split the septum for cell division and separation. Most of the PG fragments generated by these processes are taken up from the periplasm and transported to the cytoplasm by the inner membrane permease AmpG (21–25). However, in *N. gonorrhoeae*, 15% of the PG monomers escape from the cell and are released into the milieu (22). By comparison, only 4% of the PG monomers generated by *N. meningitidis* are released from the bacteria (23). We previously demonstrated that replacement of gonococcal *ampG* with meningococcal *ampG* led to reduced PG fragment release, suggesting that meningococcal AmpG is more efficient at PG fragment import (23).

In the present study, we examine the differences between gonococcal AmpG and meningococcal AmpG and characterize PG fragment release in *N. sicca* and *N. mucosa*. Replacement of meningococcal *ampG* with gonococcal *ampG* resulted in increased PG fragment release. Also, the nonpathogenic species exhibited highly-efficient PG recycling and failed to release certain PG fragments that the pathogens do release, which may indicate additional differences in PG fragment degradation, recycling, and release in nonpathogenic *Neisseria*. Overall, these data show that *Neisseria* species that are usually asymptomatic colonizers, i.e., *N. meningitidis*, *N. sicca*, and *N. mucosa*, are more efficient at PG recycling by comparison with *N. gonorrhoeae*. Thus *N. gonorrhoeae* has evolved an inefficient PG recycling system as it has moved to a proinflammatory infection lifestyle.

Journal of Bacteriology

MATERIALS AND METHODS

Bacterial strains and growth conditions. All bacterial strains used in this study are listed in Table 1. *Neisseria* strains (*N. gonorrhoeae, N. meningitidis, N. sicca* and *N. mucosa*) were grown on either gonococcal base medium (GCB) agar plates (Difco) at 37°C with 5% CO_2 or in gonococcal base liquid medium (GCBL) containing Kellogg's supplements (26) and 0.042% $NaHCO_3$ (complete GCBL or cGCBL) at 37°C with aeration. *Escherichia coli* cells were grown either on LB agar plates (Difco) at 37°C or in LB broth at 37°C with aeration. When necessary, media were supplemented with antibiotics for selection. Chloramphenicol was used at concentrations of 10 µg/ml (*Neisseria*) or 25 µg/ml (*E. coli*), while erythromycin was used at concentrations of 10 µg/ml (*Neisseria*) or 500 µg/ml (*E. coli*). Kanamycin was used at concentrations of 80 µg/ml (*Neisseria*) or 40 µg/ml (*E. coli*).

Strain construction. Mutant or complemented strains of *N. gonorrhoeae, N. meningitidis, N. sicca* and *N. mucosa* were generated using spot transformation (27). Briefly, 1 – 20 µg linearized plasmid DNA or chromosomal DNA were spotted onto GCB plates. 3-10 piliated colonies were then streaked over the spots, and the plates incubated overnight at 37°C with 5% CO_2. Transformants were screened by colony PCR and restriction enzyme digestion where applicable, and confirmed by sequencing (28).

Plasmid construction. All plasmids used in this study are listed in Table 2, while all primers used to generate the constructs are listed in Table 3. Specific details of plasmid construction are described in the supplementary methods. pIDN3 is a cloning plasmid that contains the gonococcal and meningococcal DNA uptake sequence (DUS) (GCCGTCTGAA), and was used as a vector backbone to generate most of the plasmids used in this study (29, 30). However, transformation into *N. sicca* and *N. mucosa* may have higher efficiency with an alternate DNA uptake sequence (GTCGTCTGAA), which is more commonly found in *N. sicca* ATCC 29256 and *N. mucosa* ATCC 25996 (5, 31). Thus, we constructed pEC026, a derivative of pIDN3 that contains the alternate DNA uptake sequence to be used as a vector backbone for transformations into *N. sicca* and *N. mucosa*. To facilitate screening of transformants, we introduced a silent mutation at base 993 (L331, CTG-> CTA) of gonococcal and meningococcal *ampG* to generate an *Nhe*I site. For clarity and simplicity, constructs that have WT *ampG* coding sequence are referred to as *ampG*$_{\mathrm{GC\ WT}}$ or *ampG*$_{\mathrm{MC\ WT}}$, while constructs with the screening site are referred to as *ampG*$_{\mathrm{GC}}$ or *ampG*$_{\mathrm{MC}}$.

The chimeric *ampG* constructs (pEC016-pEC019) were generated with pEC013 as a base. The *ampG* coding sequence was divided into four unequal quarters (also called *ampG* regions 1-4), in which each region contains at least one nonsynonymous nucleotide polymorphism in GC and MC. The *ampG* coding region is 1284 base pairs long. Region 1 encompassed base pairs 1-150, while region 2 contained base pairs 151-788. Region 3 is comprised of base pairs 789-992, while region 4 included base pairs 993-1284. The chimeric *ampG* constructs also contained ~600bp *ampG*$_{\mathrm{GC}}$ 5' and 3' flanking region to facilitate double crossover homologous recombination when transformed into *Neisseria.*

Characterization of released PG fragments. Metabolic labeling of PG using [6-^{3}H]-glucosamine was performed as described by Rosenthal and Dziarski (32) with modifications from Cloud and Dillard (33). Quantitative PG fragment release analysis was performed as described by Garcia and Dillard (22). Briefly, *Neisseria* strains were pulse-labeled using 10 μCi/ml [6-^{3}H]-glucosamine in GCBL lacking glucose and supplemented with 0.042% $NaHCO_3$ and pyruvate as a carbon source to label the sugar backbone, or using 25 μCi/ml [2,6-^{3}H]-diaminopimelic acid in DMEM lacking cysteine supplemented with 100 μg/ml methionine and 100 μg/ml threonine to label the peptide stems. For quantitative PG fragment release, an aliquot of the culture was removed after labeling for determination of the number of radioactive counts per minute (CPM) by liquid scintillation counting. The number of CPM was then normalized to obtain equal numbers of CPM in the bacteria in each culture. Pulse-labeling was then followed by a 2 hr (*N. meningitidis*) or 2.5 hr chase (*N. gonorrhoeae, N. sicca* and *N. mucosa*) period in cGCBL to achieve an equal number of generations. At the end of the chase period, culture supernatant was obtained by centrifugation at 3000 x *g* for 10 mins and filter-sterilization of the supernatant using a 0.22 μm pore filter. Radiolabeled PG fragments in the supernatant were separated by size using tandem size-exclusion chromatography and detected by liquid scintillation counting. Relative amounts of PG fragments released were determined by calculating the area under the curve.

Immunoblotting and detection of AmpG-FLAG3. 10 μg whole-cell lysates were electrophoresed on 12% SDS-PAGE gels. The proteins were then transferred onto polyvinylidene fluoride (PVDF) membrane (Bio-Rad) either at 100 V for 1 hr or at 20 V overnight. Membranes were blocked with 5% milk in Tris-buffered saline (TBS) for 1 hr at room temperature (RT), and then incubated with anti-FLAG® M2 primary antibody (Sigma-Aldrich) in TBS with 0.05% Tween-20 (TTBS) with 5% milk either for 1 hr at RT or overnight at 4°C. Membranes were washed 4x with TTBS for 5 mins each at RT, incubated with goat anti-mouse IgG-HRP secondary antibody (Santa Cruz) in TTBS for 1 hr, and washed 5x with TTBS for 5 mins each. Blots were developed using an Immun-Star horseradish peroxidase substrate kit (Bio-Rad), and imaged using the Odyssey® Fc Imagining System (LI-COR). Band intensities and protein concentrations were determined using Odyssey® Fc.

Quantitative RT-PCR. Quantitative RT-PCR was performed according to Salgado-Pabón (34). Briefly, gonococcal strains were grown in cGCBL until mid-log phase. RNA from 2 ml of culture was isolated using TRIzol® reagent and treated with TURBO DNAse to remove DNA contaminants (Life Technologies). Reverse transcription was then performed using the iScript cDNA synthesis kit (Bio-Rad). The resulting cDNA samples were then used for quantitative real-time PCR using the iQ SYBR Green supermix (Bio-Rad) with primers ampG-RT-F (GTGCGTGCTGCTGTTTATC) and ampG-RT-R (GTCTTGCTGAAACCCATATCC) to measure *ampG* transcript levels and primers rmp-RT-F (CGAAGGCCATACCGACTTTATGG) and rmp-RT-R (GTTGCTGACCAGGTTGTTTGC) to measure *rmp* transcript levels as a control. Rmp was chosen as a control because it is a constitutively expressed protein that is not regulated by iron levels, and *rmp* levels have been used to normalize RT-PCR data (35–37). Quantitative RT-PCR results were analyzed using the StepOnePlus™ System (Applied Biosciences). Statistical analyses were performed using Student two-tailed *t* test.

Model of gonococcal AmpG structure. The predicted structure of gonococcal AmpG was modeled using I-TASSER server (38–41) with multiple threading templates and using Phyre2 with a multi-template/*ab initio* template (42). Structures of the following proteins were used as templates for I-TASSER: *E. coli* glycerol-3-transporter GlpT (PDB ID 1PW4), MdfA multidrug transporter (PDB ID 4ZOW), *E. coli* YajR transporter (PDB ID 3WDO) and *E. coli* lactose permease LacY (PDB ID 1PV6). Structures of the following proteins were used as templates for Phyre2: human glucose transporter GLUT3/SLC2A3 (PDB ID 5C6C), *E. coli* glycerol-3-phosphate transporter GlpT (PDB ID 1PW4), *E. coli* YajR transporter (PDB ID 3WDO), *E. coli* lactose permease LacY (PDB ID 1PV7), a eukaryotic phosphate transporter (PDB ID 4J05) and a *Staphylococcus epidermidis* glucose transporter (PDB ID 4LDS).

RESULTS

Meningococcal AmpG is more efficient at PG fragment recycling compared to gonococcal AmpG. We previously generated a gonococcal strain that expresses meningococcal *ampG* (EC505) and characterized the PG fragment profile of this gene replacement mutant (23). The native gonococcal *ampG* (*ampG*$_{\mathrm{GC\ WT}}$) was replaced with meningococcal *ampG* (*ampG*$_{\mathrm{MC\ WT}}$) coding region through double crossover homologous recombination to generate EC505. Using metabolic labeling of PG with [6-^{3}H]-glucosamine and quantitative fragment release in three independent experiments, we determined that EC505 released 52% of PG monomers, and 33% disaccharide compared to wild-type (WT) *N. gonorrhoeae* (MS11) (Figure 1A and 1C) in agreement with previous observations (23). We employed a similar strategy to generate a meningococcal strain that expresses gonococcal *ampG* (EC1001), and determined EC1001 released ~39% more PG monomers compared to WT MC (ATCC 13102) (Figure 1B and 1C). The differences in the amounts of PG monomers released in the gene replacement mutants compared to WT GC and WT MC are not identical to each other, or to the differences seen between WT GC and WT MC (2.8-fold less in WT MC). This discrepancy is likely due to the increased degradation of PG fragments in MC compared to GC, as previously described (23). Our results suggest that meningococcal AmpG is more efficient at PG fragment recycling compared to gonococcal AmpG. Thus, expression of meningococcal AmpG by *N. gonorrhoeae* reduced the amount of proinflammatory PG monomers released into the extracellular milieu, and vice versa.

AmpG from gonococcal strain MS11 and meningococcal strain ATCC 13102 have 97% identity and differ only by nine amino acid residues (Figure 3A, Supplementary Figure 1). We sought to determine if the difference in PG recycling efficiency is caused by differences in *ampG* expression levels, or if small differences in protein sequence impact AmpG function. We performed quantitative RT-PCR on RNA samples isolated from WT GC (MS11), WT MC (ATCC 13102), GC expressing meningococcal *ampG* (EC505) and MC expressing gonococcal *ampG* (EC1001). If the difference in recycling efficiency is a direct consequence of differences in *ampG* expression, we would expect to see higher levels of *ampG* transcript expressed by strains that release lower levels of PG fragments, such as ATCC 13102 and EC505, compared to strains that release higher levels of PG fragments, such as MS11 and EC1001. Interestingly and contrary to this hypothesis, bacterial strains that are more efficient at recycling produced lower levels of *ampG* transcript compared to the strains that are less efficient at recycling. Gonococcal strain MS11 produced higher levels of *ampG* transcript compared to meningococcal strain ATCC 13102 (Figure 2A). EC505, which is more efficient at recycling compared to MS11 produced lower levels of *ampG* transcript compared to MS11 (Figure 2B). ATCC 13102, which is more efficient at recycling compared to EC1001, did not show increased *ampG* transcript compared to the latter strain (Figure 2C).

To determine levels of AmpG protein in WT gonococci and in WT meningococci, we raised polyclonal antibodies against a short AmpG epitope (FRREILSDEELGLG) (Genscript). Unfortunately, this antibody was not specific enough to detect AmpG levels in an immunoblot (data not shown). As an alternative, we generated strains expressing AmpG fused to a C-terminal triple FLAG tag ($(DYKDDDDK)_3$) and performed immunoblotting using anti-FLAG® M2 primary antibody. There was no significant difference in the amount of AmpG-FLAG3 expressed by WT gonococci and WT meningococci (Figure 2D and 2E). Taken together, these results suggested that the difference in PG fragment release between *N. gonorrhoeae* and *N.*

meningitidis was not due to higher *ampG* expression levels or AmpG protein levels in strains that are more efficient at recycling.

Three residues near the C-terminal end of AmpG modulate AmpG recycling efficiency. Although AmpG sequences from *N. gonorrhoeae* strain MS11 and *N. meningitidis* ATCC 13102 are 97% identical, the nine amino acid residues that differ may impact protein function. To determine which residues affect AmpG efficiency, we designed four chimeric *ampG* constructs to be expressed in *N. gonorrhoeae* (Figure 3A). We divided AmpG into four unequal regions – region 1 (N-terminal end, bp 1-150), region 2 (mid gene, closer to N-terminal end, bp 151-788), region 3 (mid gene, closer to C-terminal end, bp 789-992) and region 4 (C-terminal end, bp 993-1284) – in which each region contained at least one residue that differs between MS11 and ATCC 13102. Each chimeric gene construct is comprised of approximately one-quarter gonococcal *ampG* coding region and approximately three-quarters meningococcal *ampG* coding region, so that each chimeric protein expressed would contain a mixture of gonococcal and meningococcal AmpG residues. We would expect to see a WT GC-like phenotype for PG fragment release in strains that express the gonococcal region(s) that codes for AmpG residues important for function, while the other strains would phenocopy a strain that expresses *ampG*$_{\mathrm{MC\ WT}}$ (EC505). Only expression of a chimeric AmpG protein with meningococcal region 1-3 and gonococcal region 4 (EC511) resulted in a WT GC-like phenotype (Figure 3B). This strain showed a large increase in release of PG monomers as well as increased release of the other small PG fragments compared to strains that express the other chimeric AmpG proteins with gonococcal *ampG* regions 1, 2 or 3. We also produced a GC strain expressing *ampG* carrying gonococcal regions 1-3 and meningococcal region 4. This strain phenocopied EC505, indicating that the six changes in these three regions do not decrease AmpG function (data not shown). Our results suggest that residues in AmpG region 4 modulate AmpG efficiency.

Three residues in AmpG region 4 that differ between gonococcal and meningococcal AmpG are residues 391 (methionine in GC, leucine in MC), 398 (arginine in GC, glutamine in MC), and 402 (isoleucine in GC, alanine in MC). To determine which residues are most important for modulating AmpG function, we utilized site-directed mutagenesis to perform single, double and triple substitutions of gonococcal AmpG residues 391, 398 and 402 with the corresponding meningococcal residues. Expression of *ampG*$_{GC}^{M391L}$ and *ampG*$_{GC}^{I402A}$ reduced PG monomer release in *N. gonorrhoeae*, although not to the levels seen in the gene replacement mutant, EC505 (Figure 4A). Expression of *ampG*$_{GC}^{R398Q}$ resulted in a WT GC-like phenotype (Figure 4A).

We next asked if double substitutions of residues 391 and 402 from the gonococcal to the meningococcal residues would result in an additive effect, leading to PG monomer release levels similar to that of gonococci expressing meningococcal *ampG*. Gonococcal strains that expressed *ampG*$_{GC}^{M391L\ I402A}$ phenocopied strains that expressed the *ampG*$_{GC}^{M391L}$ and *ampG*$_{GC}^{I402A}$ single substitution mutants, releasing an intermediate level of PG monomers (Figure 4B). Double substitutions of any of the three residues resulted in PG monomer release levels similar to that of gonococcal strains expressing *ampG*$_{GC}^{M391L}$ or *ampG*$_{GC}^{I402A}$, suggesting that double mutations did not have an additive effect on PG recycling efficiency (Figure 4B). Substitutions of all three residues 391, 398 and 402 from the gonococcal to the meningococcal residues resulted in PG monomer release levels similar to that of gonococci expressing meningococcal *ampG* (Figure 4C). Our results suggested that residues 391, 398 and 402 work cooperatively to modulate AmpG function.

AmpG residues 391, 398 and 402 do not regulate levels of AmpG protein. We hypothesized that substitutions of residues 391, 398, and 402 from the gonococcal to the meningococcal variants might stabilize the protein. Thus, increased recycling efficiency in the gonococcal strain that expressed *ampG*$_{GC}^{M391L\ R398Q\ I402A}$ could be a result of increased AmpG protein levels. To test this idea, we tagged various gonococcal *ampG* substitution mutants that were more efficient at recycling compared to WT GC with the C-terminal triple FLAG epitope and measured AmpG protein levels by immunoblot. There was no significant difference in the amounts of AmpG-FLAG3 protein in any of the mutant strains tested (Figure 5). Thus, strains that expressed *ampG* variants that are more efficient at recycling PG fragments did not produce more AmpG-FLAG3 protein compared to WT gonococci. The immunoblot results suggested that substitutions of residues 391, 398, and 402 from the gonococcal to the meningococcal variants do not increase AmpG stability and levels.

***Neisseria sicca* and *Neisseria mucosa* are more efficient at PG recycling, and release lower levels of PG fragments compared to *N. gonorrhoeae*.** There are eight species of human associated, nonpathogenic *Neisseria* that asymptomatically colonize the human nasopharyngeal and oropharyngeal space. They include *N. sicca, N. mucosa, N. lactamica, N. polysaccharea, N. subflava, N. flavescens, N. cinerea* and *N. elongata* (43). We hypothesized that nonpathogenic *Neisseria* would release lower levels of PG fragments to evade immune clearance and maintain asymptomatic carriage in human hosts. We found that both *N. sicca* and *N. mucosa* released lower levels of PG monomers compared to *N. gonorrhoeae* (Figure 6). Intriguingly, both *N. sicca* and *N. mucosa* also released very small amounts or possibly no PG dimers (Figure 6).

To determine AmpG recycling efficiency in *N. sicca* and in *N. mucosa*, we compared the amounts of PG fragments released by WT and an *ampG* mutant that is unable to recycle PG fragments. We mutated *N. sicca* and *N. mucosa ampG* by interrupting the *ampG* coding sequence with a kanamycin resistance cassette. Since there are currently no complementation constructs available for *N. sicca* and *N. mucosa*, we generated backcrossed strains by transforming WT *N. sicca* and *N. mucosa* with chromosomal DNA isolated from the *ampG* deletion mutants. We calculated the recycling efficiency in *N. sicca* and *N. mucosa* by determining the area under the monomer curve for WT and *ampG* mutants. Both *N. sicca* and *N. mucosa* released 5% and recycled 95% of PG monomers liberated during PG turnover (Figure 7). This level of PG monomer release is very similar to that of *N. meningitidis*, which releases 4% of PG monomers (23). Free disaccharide release was also increased in the *N. sicca* and *N. mucosa ampG* mutants, suggesting that the permease also transports these PG molecules, in agreement with previous reports (23, 44).

Bioinformatic analyses demonstrate that all gonococci encode M391, R398, and I402 in *ampG*. We compiled and aligned *ampG* alleles expressed by 31 strains from 9 species of *Neisseria* and found that all gonococcal strains surveyed have methionine, arginine and isoleucine at AmpG positions 391, 398 and 402 (Supplementary Figure 1). A query of the sequences in the *Neisseria* Multi Locus Sequence Typing website (http://pubmlst.org/neisseria) and the Meningitis Research Foundation (MRF) Meningococcus Genome Library database (http://meningitis.org/research/genome) revealed that while no gonococcal strains (out of 1,847 sequences) had leucine, glutamine and alanine at the three positions, there were two strains of *N. polysaccharea* (out of 19 sequences) (45), eight strains of *N. lactamica* (out of 130 sequences) and around 420 meningococcal strains (out of 7,141 sequences), predominantly of the ST-269 and to a lesser extent, the ST41/44 subtypes, that had methionine, arginine and isoleucine at AmpG residues 391, 398 and 402 (data not shown). These three amino acid changes were found in 5.88% of meningococcal strains. One example each of *N. polysaccharea* (strain 12030-2014), *N. lactamica* (strain 049-12) and *N. meningitidis* (strain M10-240473) are shown in Supplementary Figure 1.

We also sequenced *ampG* from several meningococcal clinical isolates, and found an isolate, *N. meningitidis* strain NM00268, that codes for the gonococcal-like residues arginine and isoleucine at AmpG positions 398 and 402 (Supplementary Figure 1). NM00268 labels poorly with $[^3H]$-glucosamine, and thus was labeled with $[^3H]$-diaminopimelic acid instead. In accordance to our model, NM00268 released approximately 1.7 times more PG monomers compared to ATCC 13102 (Figure 8), providing support to our hypothesis that having gonococcal-like residues at AmpG positions 391, 398 and/or 402 contribute to increased PG monomer release. There were no significant differences in the amount of peptides released by NM00268 and ATCC 13102.

We constructed a neighbor-joining tree based on AmpG sequences, and found that while gonococcal strains tend to cluster together, strains of *N. lactamica* and *N. polysaccharea* that expressed GC-like AmpG residues 391, 398 and 402, did not cluster with *N. gonorrhoeae* or with each other. While *N. meningitidis* strains NM00268 and M10-240473 cluster close to each other, they did not cluster with *N. gonorrhoeae* or with *N. lactamica* strain 049-12 or *N. polysaccharea* strain 12030-2014. In addition, *N. polysaccharea* strain 12030-2014 did not cluster well with other strains from the same species, suggesting that the AmpG sequences in these non-gonococcal strains evolved independently or resulted from horizontal gene transfer events creating mosaic AmpG sequences, as is seen for *N. meningitidis* PBP2 (46). As a control, we also constructed a neighbor-joining tree based on Gdh sequences (Supplementary Figure 2). With the exception of *N. meningitidis* strain 8013, all other strains clustered with members of the same species. Overall, these results demonstrated that while M391, R398 and I402 are present in a small fraction of meningococcal or nonpathogenic *Neisseria* strains, these AmpG-crippling mutations are universally present in *N. gonorrhoeae*, making it likely that all *N. gonorrhoeae* isolates release high levels of PG fragments.

AmpG residues 391, 398 and 402 are predicted to be located on a transmembrane helix near the periplasmic face of the protein. We used I-TASSER and Phyre2 servers to predict the structure of AmpG, and obtained two different putative AmpG structures (38–42). The model of AmpG structure obtained by I-TASSER showed an inward facing conformation, in which irregularly arranged helices surround a substrate binding cavity that opens towards the cytoplasm (Figure 9A). On the other hand, the predicted structure of AmpG using Phyre2 showed an occluded conformation that may be a transitional state between the inward facing and the outward (periplasmic) facing conformations during transport (Fig 9B). In both models, AmpG residues 391, 398 and 402 are located near the periplasmic face of the protein at the start of the last transmembrane helix.

DISCUSSION

The release of PG fragments is not unique to *Neisseria,* although few genera besides *Neisseria* release mainly toxic anhydro-PG monomers. PG moieties released by bacteria have been implicated in resuscitation of dormant mycobacteria, development of *Myxococcus* fruiting bodies, germination of *Bacillus subtilis* spores and establishment of mutualism between *Bacillus cereus* and *Flavobacterium johnsoniae* (reviewed in (47), (48) and (49)). Nonetheless, the release of PG monomers by bacteria tends to lead to inflammation and death of animal host cells, whether this interaction leads to beneficial or detrimental effects at the organismal level. Tetrapeptide monomer (also known as TCT) and lipopolysaccharide (LPS) released by *Vibrio fischeri* work synergistically to induce regression of ciliated epithelial cells near the light organ of the Hawaiian bobtail squid to allow establishment of squid-*Vibrio* symbiosis (21, 50, 51). The production of PG fragments is also thought to be important for the pathogenesis of multiple bacterial species, including but not limited to human pathogens like *Helicobacter pylori* and *Shigella flexneri,* as well as plant pathogens like *Pseudomonas syringae* and *Erwinia amylovora* (reviewed in (48)).

Besides *N. gonorrhoeae*, the effects of released PG fragments on host fitness is most well studied with respect to the human pathogen *Bordetella pertussis,* which causes whooping cough. Unlike *Neisseria,* which releases a mixture of tripeptide monomer and TCT, *B. pertussis* releases exclusively TCT. TCT causes the sloughing and death of ciliated tracheal cells in *ex vivo* hamster tracheal tissue studies (14, 52, 53). An insertion element (IS*491*) ~90bp upstream of *B. pertussis ampG* reduced *ampG* expression in *B. pertussis* and results in high levels of TCT released (54). When IS*491* is deleted, or when *E. coli ampG* is expressed in *B. pertussis* instead, the amount of TCT released is significantly lowered (54). Collectively, these findings suggest that both human pathogens *B. pertussis* and *N. gonorrhoeae* evolved different strategies to reduce PG fragment recycling efficiency to release more PG monomers. This process generates an inflammatory environment that may be favorable for bacterial growth and invasion

In this work, we showed that *N. gonorrhoeae* releases more PG monomer and is less efficient at recycling PG monomers compared to *N. meningitidis*, *N. sicca* and *N. mucosa*, three species of *Neisseria* that can asymptomatically colonize the human nasopharyngeal space. With *N. gonorrhoeae* and *N. meningitidis*, the difference in the recycling efficiency is not due to higher expression of *ampG* in *N. meningitidis* compared to *N. gonorrhoeae*. In fact, gonococcal and meningococcal strains that are more efficient at recycling consistently produced lower levels of *ampG* transcript compared to strains that are less efficient at recycling. Furthermore, we did not see significant differences in the amount of various AmpG-FLAG3 proteins expressed by *N. gonorrhoeae*, and amino acid substitutions to make gonococcal AmpG more like meningococcal AmpG did not increase AmpG protein levels. These data indicated that it is not reduced amounts of *ampG* transcript or AmpG protein that makes *N. gonorrhoeae* deficient at recycling, but rather the reduced function of gonococcal AmpG in facilitating PG fragment recycling.

We also showed that reduced recycling efficiency in *N. gonorrhoeae* can be accounted for by the amino acid identity of residues 391, 398 and 402, which are close to the C-terminal end of AmpG (Figure 9). Although we do not yet understand how these three residues modulate AmpG function, beyond that the three residues do not change AmpG protein levels, we have several hypotheses. One hypothesis is that residues 391, 398, and 402 may directly bind to PG, and the gonococcal residues are either less able to bind PG fragments, or bind PG fragments too tightly, making transport of PG fragments less efficient compared to the meningococcal, *N. sicca* or *N. mucosa* AmpG counterparts.

The *E. coli* AmpG homolog is powered by proton motive force (44), although it is unknown if AmpG functions as a H^+/PG fragment symporter or if AmpG interacts with a proton transducing protein that powers the permease. It is also unknown if PG-degrading enzymes work together in a complex to remodel the PG layer, and if such complexes co-localize or interact with AmpG to ensure efficient recycling. Lytic transglycosylases are PG-degrading enzymes that cleave the glycan backbone to generate PG monomers (20). *N. gonorrhoeae* has two lytic transglycosylases, LtgA and LtgD, that generate all or nearly all the PG monomers released by the bacterium. Deletion of *ltgD* leads to a larger reduction in the amount of PG monomers released compared to deletion of *ltgA* (62% reduction vs 38% reduction) (19). However, LtgA generates more PG monomers than LtgD and LtgA-generated monomers are preferentially taken up into the cytoplasm for recycling (55). Thus, it is also possible that residues 391, 398 and 402 facilitate protein-protein interaction with hypothetical accessory protein(s), or with PG-degrading enzymes like LtgA in the periplasm to power AmpG function or ensure efficient PG recycling.

Another hypothesis is that the residues at these positions are important for facilitating conformational changes required for the import of PG fragments into the cytoplasm. AmpG belongs to major facilitator superfamily (MFS). MFS proteins are typically membrane transport proteins with 12 or 14 transmembrane α-helices that can function as uniporters, symporters and antiporters and can be found in bacteria, eukaryotes and archaea (56, 57). The most well-studied MFS protein, LacY, is a lactose/H^+ symporter that can assume one of at least two conformations, as determined by X-ray crystallography studies. LacY can assume a conformation with two-fold pseudosymmetry with a large aqueous, substrate-binding cavity that opens towards the cytoplasm (PDB ID 1PV7, 2V8N) (58, 59). It is proposed that LacY can assume a similar conformation in which the aqueous cavity opens towards the periplasm for substrate binding

(60). LacY can also form an occluded conformation with a narrow cavity that opens slightly towards the periplasm that is thought to be an intermediate conformation during substrate transport (PDB ID 4OAA, 4ZYR) (61, 62). Given that the two predicted AmpG structures resembled the two structurally determined conformations of LacY, AmpG may function similarly to LacY. As such, residues at positions 391, 398 and 402 might impact the rate of conformational changes required for transport. The crystal structure of AmpG and the exact mechanism of action that AmpG uses to transport PG fragments are currently unknown. A crystal structure of AmpG would help inform studies of AmpG's mechanism of action and provide insight into how residues 391, 398 and 402 impact AmpG efficiency.

We hypothesize that the differences in AmpG function and PG fragment release between the asymptomatic colonizers and *N. gonorrhoeae* contribute to the differences in the inflammatory responses to these species at their different infection sites. It should be noted that *ampG* is not the only factor affecting PG fragment release. Comparing *N. meningitidis* to *N. gonorrhoeae*, expression of meningococcal *ampG* in gonococci results in a near two-fold decrease in PG release, but expression of gonococcal *ampG* in meningococci only resulted in a 39% increase in PG monomer release (Figure 1). These results suggest that additional features of PG fragment metabolism in *N. gonorrhoeae* may favor PG fragment release, and that *N. meningitidis* and the nonpathogenic *Neisseria* species may have additional mechanisms for increasing PG fragment recycling and diminishing PG fragment release. Increased PG fragment breakdown by *N. meningitidis* as well as *N. mucosa* and *N. sicca* as compared to *N. gonorrhoeae* can be seen in the PG fragment release profiles (Figure 1, Figure 6) (23). Less PG dimers and monomers are released but more anhMurNAc is released as compared to *N. gonorrhoeae*. In addition to the reduced PG fragment release we have shown here, nonpathogenic *Neisseria* are also known to produce a lipid A structure that is less inflammatory (6). Together with differences in the responsiveness of the different tissues infected by these species, the differences in lipid A and PG fragment release may explain how nonpathogenic *Neisseria* are able to maintain asymptomatic colonization while *N. gonorrhoeae* usually induces a strong inflammatory response and disease.

ACKNOWLEDGEMENTS

We thank Nate Weyand for the gift of *N. sicca* ATCC 29256 and *N. mucosa* ATCC 25996. We are grateful to Katie Hackett, Jon Lenz and Ryan Schaub for experimental support and discussions.

FIGURE LEGENDS

Figure 1. Expression of non-native *Neisseria ampG* in *N. gonorrhoeae* and *N. meningitidis* altered peptidoglycan fragment release. Released [^{3}H]-glucosamine labeled PG fragments were separated by size-exclusion chromatography and detected by liquid scintillation counting to generate a PG fragment release profile. Symbols for PG sugars and amino acids are based on Jacobs *et al*. (24). A) Comparison of WT GC (MS11, dark grey line) to a gonococcal *ampG* replacement mutant expressing $\mathit{ampG}_{\mathrm{MC\ WT}}$ (EC505, light grey line). B) Comparison of WT MC (ATCC 13102, dark grey line) to a meningococcal *ampG* replacement mutant expressing $\mathit{ampG}_{\mathrm{GC\ WT}}$ (EC1001, light grey line). C) Quantification of the amount of PG fragments released by the *ampG* replacement mutants compared to WT in three independent experiments. *

indicates that the amount of PG fragments released by the gene replacement mutant was significantly different compared to WT by Student two-tailed *t* test ($p<0.05$).

Figure 2. *Neisseria* strains that were more efficient at recycling PG fragments did not express higher levels of *ampG*. Transcript levels for *ampG* were determined comparing: A) WT MC (ATCC 13102) to WT GC (MS11), B) $ampG_{\mathrm{GC\ WT}}^{-}$ $ampG_{\mathrm{MC\ WT}}^{+}$ (EC505) to WT GC, and C) WT MC to $ampG_{\mathrm{MC\ WT}}^{-}$ $ampG_{\mathrm{GC\ WT}}^{+}$ (EC1001). RT-PCR results are from three biological replicates with technical triplicates. D) Protein levels of AmpG-FLAG3 were determined for GC and MC strains by Western blot. WT gonococci and meningococci that did not express FLAG3 tagged AmpG protein were included as negative controls. E) Quantification of the AmpG-FLAG3 bands from three independent experiments was performed using LiCor Odyssey Fc. Statistical significance was determined using Student two-tailed *t* test. * indicates statistical significance, with $p<0.05$, while n.s. indicates not significant.

Figure 3. Residues near the C-terminal end of AmpG (AmpG region 4) modulated AmpG recycling efficiency. A) Cartoon depiction of the AmpG replacement and AmpG chimera constructs expressed in *N. gonorrhoeae* (not to scale). The AmpG replacement construct (top) was used as a base to generate the chimera constructs. Residues that differ between GC AmpG and MC AmpG are indicated in this format: [gonococcal residue][residue number][meningococcal residue]. Each chimera construct contained approximately one-quarter gonococcal *ampG* coding region and three-quarters meningococcal *ampG* coding region, and contained a mixture of gonococcal and meningococcal residues. B) PG fragment release profiles for *N. gonorrhoeae* strains expressing different versions of *ampG*.

Figure 4. AmpG residues 391, 398 and 402 worked cooperatively to modulate AmpG recycling efficiency. PG fragment release profiles are shown for: A) Single substitutions of AmpG residues 391, 398 and 402 (EC515, EC516, EC517) compared to the whole gene replacement mutant (EC505) and wild type (MS11), B) Double substitutions of AmpG residues 391, 398 and 402 (EC518, EC519, EC521) compared to WT and EC505, and C) Triple substitutions of AmpG residues 391, 398 and 402 (EC523) compared to WT and EC505.

Figure 5. Increased recycling efficiency of gonococcal *ampG* mutants was not a consequence of increased AmpG protein levels. A) AmpG was tagged with a C-terminal triple FLAG (FLAG3) epitope to determine AmpG levels made by *N. gonorrhoeae* via immunoblotting, comparing the levels of AmpG-FLAG3 expressed by different *ampG* mutant strains that have GC WT-like (EC512) or more efficient PG recycling (EC546, EC548, EC550). B) Quantification of band intensities from three independent experiments using LiCor Odyssey Fc.

Figure 6. PG fragment release from nonpathogenic *N. sicca* (ATCC 29256, green line) and *N. mucosa* (ATCC 25996, blue line) compared to *N. gonorrhoeae* (MS11, red line).

Figure 7. *N. sicca and N. mucosa* possess functional AmpG proteins. PG fragment release was examined for mutants carrying a kanamycin resistance cassette interrupting *ampG* in *N. sicca* (EC2004) (A) and *N. mucosa* (EC2003) (B) (dark grey lines) compared to WT *N. sicca* and *N. mucosa* (black lines). PG fragment release profiles for backcrossed mutants

(EC2004BC/EC2003BC, light grey lines) are also shown. Quantification of the peaks was performed with data obtained from three independent experiments.

Figure 8. PG fragment release from a meningococcal strain with naturally-occurring GC-like AmpG residues 398 and 402 (NM00268). ATCC 13102 and NM00268 were labeled with [^{3}H]-diaminopimelic acid, which labels the peptide stem of PG fragments. Quantification of the area under the curve was performed with data from three independent experiments.

Figure 9. Prediction of gonococcal AmpG structure. The predicted structure of gonococcal AmpG was determined using I-TASSER server with multiple threading templates (A) and using Phyre2 with a multi-template/*ab initio* template (B). Side view (left), and the view from the periplasmic face (right) of the AmpG structure are shown here, with residues 391, 398 and 402 displayed as dark red sticks. Residues 391, 398 and 402 are located close to the periplasmic face of the protein.

REFERENCES

1. **Dewhirst FE**, **Chen T**, **Izard J**, **Paster BJ**, **Tanner ACR**, **Yu WH**, **Lakshmanan A**, **Wade WG**. 2010. The human oral microbiome. J Bacteriol **192**:5002–5017.
2. **Zaura E**, **Keijser BJ**, **Huse SM**, **Crielaard W**. 2009. Defining the healthy "core microbiome" of oral microbial communities. BMC Microbiol **9**:259. doi: 10.1186/1471-2180-9-259.
3. **Liu G**, **Tang CM**, **Exley RM**. 2015. Non-pathogenic *Neisseria*: members of an abundant, multi-habitat, diverse genus. Microbiology **161**:1297–1312.
4. **Johnson AP**. 1983. The pathogenic potential of commensal species of *Neisseria*. J Clin Pathol **36**:213–23.
5. **Marri PR**, **Paniscus M**, **Weyand NJ**, **Rendon MA**, **Calton CM**, **Hernandez DR**, **Higashi DL**, **Sodergren E**, **Weinstock GM**, **Rounsley SD**, **So M**. 2010. Genome sequencing reveals widespread virulence gene exchange among human *Neisseria* species. PLoS One **5**:e11835. doi: 10.1371/journal.pone.0011835.
6. **John CM**, **Liu M**, **Phillips NJ**, **Yang Z**, **Funk CR**, **Zimmerman LI**, **Griffiss M**, **Stein DC**, **Jarvis GA**. 2012. Lack of lipid A pyrophosphorylation and functional *lptA* reduces inflammation by *Neisseria* commensals. Infect Immun **80**:4014–4026.
7. **Mayor MT**, **Roett MA**, **Uduhiri KA**. 2012. Diagnosis and management of gonococcal infections. Am Fam Physician **86**:931–938.
8. **Melly MA**, **McGee ZA**, **Rosenthal RS**. 1984. Ability of monomeric peptidoglycan fragments from *Neisseria gonorrhoeae* to damage human Fallopian-tube. J Infect Dis **149**:378–386.
9. **McGee ZA**, **Jensen RL**, **Clements CM**, **Taylor-Robinson D**, **Johnson AP**, **Gregg CR**.

1999. Gonococcal infection of human Fallopian tube mucosa in organ culture: relationship of mucosal tissue TNF- α concentration to sloughing of ciliated cells. Sex Transm Dis **26**:160–165.

10. **Rosenthal RS**. 1979. Release of soluble peptidoglycan from growing gonococci: hexaminidase and amidase activities. Infect Immun **24**:869–878.

11. **Sinha RK**, **Rosenthal RS**. 1980. Release of soluble peptidoglycan from growing gonococci: Demonstration of anhydro-muramyl-containing fragments. Infect Immun **29**:914–925.

12. **Rosenthal RS**, **Nogami W**, **Cookson BT**, **Goldman WE**, **Folkening WJ**. 1987. Major fragment of soluble peptidoglycan released from growing *Bordetella pertussis* is tracheal cytotoxin. Infect Immun **55**:2117–2120.

13. **Goldman WE**, **Klapper DG**, **Baseman JB**. 1982. Detection, isolation, and analysis of a released *Bordetella pertussis* product toxic to cultured tracheal cells. Infect Immun **36**:782–794.

14. **Cookson BT**, **Cho H**, **Herwaldt LA**, **Goldman WE**. 1989. Biological activities and chemical composition of purified tracheal cytotoxin of *Bordetella pertussis*. Infect Immun **57**:2223–2229.

15. **Girardin SE**, **Boneca IG**, **Carneiro LAM**, **Antignac A**, **Jehanno M**, **Viala J**, **Tedin K**, **Taha M-K**, **Labigne A**, **Zahringer U**, **Coyle AJ**, **DiStefano PS**, **Bertin J**, **Sansonetti PJ**, **Philpott DJ**. 2003. Nod1 detects a unique muropeptide from Gram-negative bacterial peptidoglycan. Science **300**:1584–1587.

16. **Stephens DS**, **Greenwood B**, **Brandtzaeg P**. 2007. Epidemic meningitis, meningococcaemia, and *Neisseria meningitidis*. Lancet **369**:2196–2210.

17. **Centers for Disease Control and Prevention**. 2015. Meningococcal Disease: Technical & Clinical Information. Accessed April 3, 2016 at http://www.cdc.gov/meningococcal/clinical-info.html.

18. **Loh E**, **Kugelberg E**, **Tracy A**, **Zhang Q**, **Gollan B**, **Ewles H**, **Chalmers R**, **Pelicic V**, **Tang CM**. 2013. Temperature triggers immune evasion by *Neisseria meningitidis*. Nature **502**:237–40.

19. **Cloud-Hansen KA**, **Hackett KT**, **Garcia DL**, **Dillard JP**. 2008. *Neisseria gonorrhoeae* uses two lytic transglycosylases to produce cytotoxic peptidoglycan monomers. J Bacteriol **190**:5989–5994.

20. **Chan YA**, **Hackett KT**, **Dillard JP**. 2012. The lytic transglycosylases of *Neisseria gonorrhoeae*. Microb Drug Resist **18**:271–279.

21. **Adin DM**, **Engle JT**, **Goldman WE**, **McFall-Ngai MJ**, **Stabb E V**. 2009. Mutations in *ampG* and lytic transglycosylase genes affect the net release of peptidoglycan monomers from *Vibrio fischeri*. J Bacteriol **191**:2012–2022.

22. **Garcia DL**, **Dillard JP**. 2008. Mutations in *ampG* or *ampD* affect peptidoglycan fragment release from *Neisseria gonorrhoeae*. J Bacteriol **190**:3799–3807.

23. **Woodhams KL**, **Chan JM**, **Lenz JD**, **Hackett KT**, **Dillard JP**. 2013. Peptidoglycan fragment release from *Neisseria meningitidis*. Infect Immun **81**:3490–3498.

24. **Jacobs C**, **Huang L**, **Bartowsky E**, **Normark S**, **Park JT**. 1994. Bacterial cell wall recycling provides cytosolic muropeptides as effectors for beta-lactamase induction. EMBO J **13**:4684–4694.

25. **Korfmann G**, **Sanders CC**. 1989. *ampG* is essential for high-level expression of AmpC beta-lactamase in *Enterobacter cloacae*. Antimicrob Agents Chemother **33**:1946–1951.

26. **Kellogg DS**, **Peacock WL**, **Deacon WE**, **Brown L**, **Pirkle CI**. 1963. *Neisseria gonorrhoeae*: Virulence genetically linked to clonal variation. J Bacteriol **85**:1274–1279.

27. **Dillard JP**. 2011. Genetic manipulation of *Neisseria gonorrhoeae*Current Protocols in Microbiology. Curr Protoc Microbiol. Chapter 4: Unit4A.2. doi: 10.1002/9780471729259.mc04a02s23.

28. **Wright CJ**, **Jerse AE**, **Cohen MS**, **Cannon JG**, **Seifert HS**. 1994. Nonrepresentative PCR amplification of variable gene sequences in clinical specimens containing dilute, complex mixture of microorganisms. J Clin Microbiol **32**:464–468.

29. **Goodman SD**, **Scocca JJ**. 1988. Identification and arrangement of the DNA sequence recognized in specific transformation of *Neisseria gonorrhoeae*. Proc Natl Acad Sci U S A **85**:6982–6986.

30. **Hamilton HL**, **Schwartz KJ**, **Dillard JP**. 2001. Insertion-duplication mutagenesis of *Neisseria*: Use in characterization of DNA transfer genes in the gonococcal genetic island. J Bacteriol **183**:4718–4726.

31. **Frye SA**, **Nilsen M**, **Tonjum T**, **Ambur OH**. 2013. Dialects of the DNA Uptake Sequence in *Neisseriaceae*. PLoS Genet **9**:e1003458. doi: 10.1371/journal.pgen.1003458.

32. **Rosenthal RS**, **Dziarski R**. 1994. Isolation of peptidoglycan and soluble peptidoglycan fragments. Methods Enzymol **235**:253–285.

33. **Cloud KA**, **Dillard JP**. 2002. A lytic transglycosylase of *Neisseria gonorrhoeae* is involved in peptidoglycan-derived cytotoxin production. Infect Immun **70**:2752–2757.

34. **Salgado-Pabón W**, **Du Y**, **Hackett KT**, **Lyons KM**, **Arvidson CG**, **Dillard JP**. 2010. Increased expression of the type IV secretion system in piliated *Neisseria gonorrhoeae* variants. J Bacteriol **192**:1912–1920.

35. **Shaik YB**, **Grogan S**, **Davey M**, **Sebastian S**, **Goswami S**, **Szmigielski B**, **Genco CA**. 2007. Expression of the iron-activated *nspA* and *secY* genes in *Neisseria meningitidis* group B by Fur-dependent and -independent mechanisms. J Bacteriol **189**:663–669.

36. **Agarwal S**, **King CA**, **Klein EK**, **Soper DE**, **Rice PA**, **Wetzler LM**, **Genco CA**. 2005. The gonococcal Fur-regulated *tbpA* and *tbpB* genes are expressed during natural mucosal gonococcal infection. Infect Immun **73**:4281–4287.

37. **Grifantini R**, **Sebastian S**, **Frigimelica E**, **Draghi M**, **Bartolini E**, **Muzzi A**, **Rappuoli R**, **Grandi G**, **Genco CA**. 2003. Identification of iron-activated and -repressed Fur-dependent genes by transcriptome analysis of *Neisseria meningitidis* group B. Proc Natl Acad Sci U S A **100**:9542–9547.

38. **Zhang Y**. 2008. I-TASSER server for protein 3D structure prediction. BMC Bioinformatics **9**:40. doi: 10.1186/1471-2105-9-40.

39. **Roy A**, **Kucukural A**, **Zhang Y**. 2010. I-TASSER: a unified platform for automated protein structure and function prediction. Nat Protoc **5**:725–738.

40. **Yang J**, **Zhang Y**. 2015. I-TASSER server: new development for protein structure and function predictions. Nucleic Acids Res **43**:W174–181. doi: 10.1093/nar/gkv342.

41. **Yang J**, **Yan R**, **Roy A**, **Xu D**, **Poisson J**, **Zhang Y**. 2015. The I-TASSER Suite: Protein structure and function prediction. Nat Methods **12**:7–8.

42. **Kelley LA**, **Mezulis S**, **Yates CM**, **Wass MN**, **Sternberg MJE**. 2015. The Phyre2 web portal for protein modelling, prediction, and analysis. Nat Protoc **10**:845–858.

43. **Tønjum T**. 2015. *Neisseria*. Bergey's Man Syst Archaea Bact 1–48.

44. **Cheng Q**, **Park JT**. 2002. Substrate specificity of the AmpG permease required for recycling of cell wall anhydro-muropeptides. J Bacteriol **184**:6434–6436.

45. **Jolley KA**, **Maiden MCJ**. 2010. BIGSdb: Scalable analysis of bacterial genome variation at the population level. BMC Bioinformatics **11**:595. doi: 10.1186/1471-2105-11-595.

46. **Bowler LD**, **Zhang QY**, **Riou JY**, **Spratt BG**. 1994. Interspecies recombination between the *penA* genes of *Neisseria meningitidis* and commensal *Neisseria* species during the emergence of penicillin resistance in *N. meningitidis*: Natural events and laboratory simulation. J Bacteriol **176**:333–337.

47. **Bertsche U**, **Mayer C**, **Götz F**, **Gust AA**. 2015. Peptidoglycan perception — Sensing bacteria by their common envelope structure. Int J Med Microbiol **305**:217–223.

48. **Cloud-Hansen KA**, **Peterson SB**, **Stabb E V**, **Goldman WE**, **McFall-Ngai MJ**, **Handelsman J**. 2006. Breaching the great wall: peptidoglycan and microbial interactions. Nat Rev Microbiol **4**:710–716.

49. **Dworkin J**. 2014. The medium is the message: interspecies and interkingdom signaling by peptidoglycan and related bacterial glycans. Annu Rev Microbiol **68**:137–154.

50. **Koropatnick TA**, **Engle JT**, **Apicella MA**, **Stabb EV**, **Goldman WE**, **McFall-Ngai MJ**. 2004. Microbial factor-mediated development in a host-bacterial mutualism. Science **306**:1186–1188.

51. **Troll JV**, **Adin DM**, **Wier AM**, **Paquette N**, **Silverman N**, **Goldman WE**, **Stadermann FJ**, **Stabb EV**, **McFall-Ngai MJ**. 2009. Peptidoglycan induces loss of a nuclear peptidoglycan recognition protein during host tissue development in a beneficial animal-bacterial symbiosis. Cell Microbiol **11**:1114–1127.

52. **Cole PJ**, **Wilson R**. 1994. Effect of tracheal cytotoxin from *Bordetella pertussis* on human neutrophil function *in vitro*. Infect Immun **62**:639–643.

53. **Luker KE**, **Tyler AN**, **Marshall GR**, **Goldman WE**. 1995. Tracheal cytotoxin structural

requirements for respiratory epithelial damage in pertussis. Mol Microbiol **16**:733–743.

54. **Lyon RS**. 2001. Tracheal cytotoxin production by the *Bordetellae*. Ph.D. thesis. Washington University in St. Louis, St. Louis, MO.

55. **Schaub RE**, **Chan YA**, **Lee M**, **Hesek D**, **Mobashery S**, **Dillard JP**. 2016. Lytic transglycosylases LtgA and LtgD perform distinct roles in remodeling, recycling, and releasing peptidoglycan in *Neisseria gonorrhoeae*. Submitted.

56. **Reddy VS**, **Shlykov MA**, **Castillo R**, **Sun EI**, **Saier MH**. 2012. The major facilitator superfamily (MFS) revisited. FEBS J **279**:2022–2035.

57. **Yan N**. 2015. Structural biology of the major facilitator superfamily transporters. Annu Rev Biophys **44**:257–283.

58. **Abramson J**, **Smirnova I**, **Kasho V**, **Verner G**, **Kaback HR**, **Iwata S**. 2003. Structure and mechanism of the lactose permease of *Escherichia coli*. Science **301**:610–615.

59. **Guan L**, **Mirza O**, **Verner G**, **Iwata S**, **Kaback HR**. 2007. Structural determination of wild-type lactose permease. Proc Natl Acad Sci United States **104**:15294–15298.

60. **Smirnova I**, **Kasho V**, **Choe J-Y**, **Altenbach C**, **Hubbell WL**, **Kaback HR**. 2007. Sugar binding induces an outward facing conformation of LacY. Proc Natl Acad Sci U S A **104**:16504–16509.

61. **Kumar H**, **Kasho V**, **Smirnova I**, **Finer-Moore JS**, **Kaback HR**, **Stroud RM**. 2014. Structure of sugar-bound LacY. Proc Natl Acad Sci United States **111**:1784–1788.

62. **Kumar H**, **Finer-Moore JS**, **Kaback HR**, **Stroud RM**. 2015. Structure of LacY with an α-substituted galactoside: Connecting the binding site to the protonation site. Proc Natl Acad Sci U S A **112**:9004–9009.

63. **Swanson J**. 1972. Studies on gonococcus infection. II. Freeze-fracture, freeze-etch studies

on gonococci. J Exp Med **136**:1258–1271.

64. **Woodhams KL**, **Benet ZL**, **Blonsky SE**, **Hackett KT**, **Dillard JP**. 2012. Prevalence and detailed mapping of the gonococcal genetic island in *Neisseria meningitidis*. J Bacteriol **194**:2275–2285.

65. **Mehr IJ**, **Long CD**, **Serkin CD**, **Seifert HS**. 2000. A homologue of the recombination-dependent growth gene, *rdgC*, is involved in gonococcal pilin antigenic variation. Genetics **154**:523–532.

Table 1. Strains used in this study.

Strain	Description	Reference or source
N. gonorrhoeae		
MS11	WT *N. gonorrhoeae*	(63)
EC505	*ampG*$_{GC}^{-}$ *ampG*$_{MC\ WT}^{+}$	(23)
EC508	MS11 transformed with pEC016; *ampG*$_{GC}^{-}$ *ampG*$_{GC\ Chimera\ 1}^{+}$	This work
EC509	MS11 transformed with pEC017; *ampG*$_{GC}^{-}$ *ampG*$_{GC\ Chimera\ 2}^{+}$	This work
EC510	MS11 transformed with pEC018; *ampG*$_{GC}^{-}$ *ampG*$_{GC\ Chimera\ 3}^{+}$	This work
EC511	MS11 transformed with pEC019; *ampG*$_{GC}^{-}$ *ampG*$_{GC\ Chimera\ 4}^{+}$	This work
EC512	MS11 transformed with pEC028; *ampG*$_{GC\ WT}$-FLAG3	This work
EC515	MS11 transformed with pEC037; *ampG*$_{GC}^{M391L}$	This work
EC516	MS11 transformed with pEC038; *ampG*$_{GC}^{R398Q}$	This work
EC517	MS11 transformed with pEC039; *ampG*$_{GC}^{I402A}$	This work
EC518	MS11 transformed with pEC042; *ampG*$_{GC}^{M391L\ R398Q}$	This work
EC519	MS11 transformed with pEC043; *ampG*$_{GC}^{M391L\ I402A}$	This work
EC521	MS11 transformed with pEC054; *ampG*$_{GC}^{R398Q\ I402A}$	This work
EC523	MS11 transformed with pEC058; *ampG*$_{GC}^{M391L\ R398Q\ I402A}$	This work
EC546	MS11 transformed with pEC100; *ampG*$_{GC}^{M391L}$-FLAG3	This work
EC548	MS11 transformed with pEC102; *ampG*$_{GC}^{I402M}$-FLAG3	This work
EC549	MS11 transformed with pEC103; *ampG*$_{GC}^{M391L\ R398Q\ I402M}$-FLAG3	This work
EC550	MS11 transformed with pEC098; *ampG*$_{GC}^{-}$ *ampG*$_{MC\ WT}$-FLAG^{+}	This work
N. meningitidis		
ATCC 13102 *cap*$^{-}$	ATCC 13102 *rpsL* (K43R) *siaD::cat* (WT *N. meningitidis*)	(23)
NM00268	Serogroup B clinical isolate	(64)
EC1001	ATCC 13102 *cap*$^{-}$ transformed with pEC008; *ampG*$_{MC}^{-}$ *ampG*$_{GC\ WT}^{+}$	This work
EC1008	ATCC 13102 *cap*$^{-}$ transformed with pEC029; *ampG*$_{MC\ WT}$-FLAG3	This work
N. sicca		
ATCC 29256	Pharyngeal mucosa isolate (WT *N. sicca*)	N. Weyand
EC2004	ATCC 29256 transformed with pEC081; *ampG*$_{N.\ sicca}$::*kan*	This work
EC2004BC	ATCC 29256 transformed with EC2004 chromosomal DNA; *ampG*$_{N.\ sicca}$::*kan* backcross	This work
N. mucosa		
ATCC 25996	Pharyngeal mucosa isolate (WT *N. mucosa*)	N. Weyand
EC2003	ATCC 25996 transformed with pEC070; *ampG*$_{N.\ mucosa}$::*kan*	This work
EC2003BC	ATCC 25996 transformed with EC2003 chromosomal DNA; *ampG*$_{N.\ mucosa}$::*kan*	This work

Table 2. Plasmids used in this study.

Plasmid	Description	Reference or source
pIDN3	Cloning plasmid containing GC/MC DNA uptake sequences	(30)
pHSS6	Cloning plasmid, source of *kanR*	(65)
pEC026	pIDN3 containing *N. sicca/N.mucosa* DNA uptake sequences	This work
pEC005	*ampG*$_{\mathrm{MC}}$*p*-*ampG*$_{\mathrm{GC\ WT}}$ cloned into pIDN3	This work
pEC006	*ampG*$_{\mathrm{GC}}$*p*-*ampG*$_{\mathrm{MC\ WT}}$ cloned into pIDN3	(23)
pEC007	*ampG*$_{\mathrm{GC}}$*p*-*ampG*$_{\mathrm{GC}}$ cloned into pIDN3	This work
pEC008	*ampG*$_{\mathrm{MC}}$*p*-*ampG*$_{\mathrm{GC}}$ cloned into pIDN3	This work
pEC013	*ampG*$_{\mathrm{GC}}$*p* *ampG*$_{\mathrm{MC}}$ cloned into pIDN3	This work
pEC016	*ampG*$_{\mathrm{GC}}$*p* *ampG*$_{\mathrm{Chimera\ 1}}$ cloned into pIDN3	This work
pEC017	*ampG*$_{\mathrm{GC}}$*p* *ampG*$_{\mathrm{Chimera\ 2}}$ cloned into pIDN3	This work
pEC018	*mpG*$_{\mathrm{GC}}$*p* *ampG*$_{\mathrm{Chimera\ 3}}$ cloned into pIDN3	This work
pEC019	*ampG*$_{\mathrm{GC}}$*p* *ampG*$_{\mathrm{Chimera\ 4}}$ cloned into pIDN3	This work
pEC028	*ampG*$_{\mathrm{GC}}$-FLAG3 cloned into pIDN3	This work
pEC029	*ampG*$_{\mathrm{MC}}$-FLAG3 cloned into pIDN3	This work
pEC037	*ampG*$_{\mathrm{GC}}$*p*-*ampG*$_{\mathrm{GC}}^{\mathrm{M391L}}$ cloned into pIDN3	This work
pEC038	*ampG*$_{\mathrm{GC}}$*p*-*ampG*$_{\mathrm{GC}}^{\mathrm{R398Q}}$ cloned into pIDN3	This work
pEC039	*ampG*$_{\mathrm{GC}}$*p*-*ampG*$_{\mathrm{GC}}^{\mathrm{I402A}}$ cloned into pIDN3	This work
pEC042	*ampG*$_{\mathrm{GC}}$*p*-*ampG*$_{\mathrm{GC}}^{\mathrm{M391L\ R398Q}}$ cloned into pIDN3	This work
pEC043	*ampG*$_{\mathrm{GC}}$*p*-*ampG*$_{\mathrm{GC}}^{\mathrm{M391L\ I402A}}$ cloned into pIDN3	This work
pEC054	*ampG*$_{\mathrm{GC}}$*p*-*ampG*$_{\mathrm{GC}}^{\mathrm{R398Q}}$ I402A cloned into pIDN3	This work
pEC058	*ampG*$_{\mathrm{GC}}$*p*-*ampG*$_{\mathrm{GC}}^{\mathrm{M391L}}$ cloned into pIDN3	This work
pEC063	*ampG*$_{\mathit{N.\ sicca}}$ cloned into pEC026	This work
pEC064	*ampG*$_{\mathit{N.\ mucosa}}$ cloned into pIDN3	This work
pEC067	*ampG*$_{\mathit{N.\ mucosa}}$::*kan* cloned into pIDN3	This work
pEC070	*ampG*$_{\mathit{N.\ mucosa}}$::*kan* cloned into pEC026	This work
pEC081	*ampG*$_{\mathit{N.\ sicca}}$::*kan* cloned into pEC026	This work
pEC098	*ampG*$_{\mathrm{MC\ WT}}$-FLAG3 cloned into pIDN3	This work
pEC100	*ampG*$_{\mathrm{GC}}^{\mathrm{M391L}}$-FLAG3 cloned into pIDN3	This work
pEC102	*ampG*$_{\mathrm{GC}}^{\mathrm{I402A}}$-FLAG3 cloned into pIDN3	This work
pEC103	*ampG*$_{\mathrm{GC}}^{\mathrm{M391L\ R398Q\ I402A}}$-FLAG3 cloned into pIDN3	This work

Table 3. Primers used in this study.

Primer name	Sequence (5' to 3')
MC ampG sacI F3	ATTCAGAGCTCCATCGGCGGCATCATCAAAC
SacI ampG F	CGGGAGCTCGCGATATTTGCTACAATAGGC
XbaI ampG R	GCCCTCTAGACACAATATCAGGTAAACGCTCC
ampG 5' flank R	AGCCTATTGTAGCAAATATCGCC
ampG F2	GGCGATATTTGCTACAATAGGCT
ampG 3' flank F	TCAAACTGGAGCGTTTACCTGATATTG
ampG1325R	CAATATCAGGTAAACGCTCCAGTTTGA
ampG 3' flank R BamHI	CTCAGGATCCGTTCTTTATATGAGCGGCAGG
ampG 990bp NheI F	GTAAGCTAGCGGCAGTTATCGGCGCGGAAG
ampG 990bp NheI R	CTAAGCTAGCATCAGCCTCTCGCCTGTG
ampG internal 1 F	CAGCGAGCAGGTGGATTTGAAG
ampG internal 1 R	CTTCAAATCCACCTGCTCGCTG
ampG internal 2 F	GGATATGGGTTTCAGCAAGAC
ampG internal 2 R	GTCTTGCTGAAACCCATATCC
Alt-DUS AvrII F	GGCTGCCTAGGTTCAGACGACAAGCTAATT
Alt-DUS AvrII R	GGTTGCCTAGGTTCAGACGACATGCAGC
ampG-FLAG3 F	CAGGCAGAGGTTCCGCTGGCTCCGCT
ampGend-FLAG3 R	CCTGCATCCTTATGAGAAAGTAAGTTC
(Gc) FLAG3-ampGend F	TTCTCATAAGAGAAAACCCAGGATGCAGG
(Gc) FLAG3-ampGend R	AGCGGAACCTCTGCCTGCATCCTGGG
(Mc) FLAG3-ampGend F	TTCTCATAAGAGAAAACTCAGGATGCAGG
(Mc) FLAG3-ampGend R	AGCGGAACCTCTGCCTGCATCCTGAG
MS11 AmpG R398Q F	GTACCGTTTTTCCAGTTGTGTTTCATAC
MS11 AmpG R398Q R	GTATGAAACACAACTGGAAAAACGGTAC
MS11 AmpG M391L F	CTGATCGAATGGCTGGGTTATGTACCG
MS11 AmpG M391L R	CGGTACATAACCCAGCCATTCGATCAG
MS11 AmpG I402A F	GGCTGTGTTTCGCACTTGCCCTG
MS11 AmpG I402A R	CAGGGCAAGTGCGAAACACAGCC
MS11 AmpG R398Q I402A F	CAGTTGTGTTTCGCACTTGCCCTG
MS11 AmpG R398Q I402A R	CAGGGCAAGTGCGAAACACAACTG
NSi ampG SacIF	CAGGAGAGCTCGTACTGCTCATCCATTATGAC
NSi ampG down BamHI R2	CATTAGGATCCCAATCGGCGTGTCTGCGATG
NMu ampG SacIF	CGCCGAGAGCTCGATGTTGTTCTCCCATTATGAC
Nmu ampG BamHI R	GACGAGGATCCCTACCGATACATTCAAACG
rmp-RT-F	CGAAGGCCATACCGACTTTATGG
rmp-RT-R	GTTGCTGACCAGGTTGTTTGC
ampG-RT-F	GTGCGTGCTGCTGTTTATC
ampG-RT-R	GTCTTGCTGAAACCCATATCC
gdh-F2	GTAGCGATGAGTAGTATTAC
gdh-R1	GCCGTACTATTTGTACTGTC
gdh-R2	GTGATTTCAGACGGCATATC
gdh-internal-F	GGCAAAGAAAGCCTGC

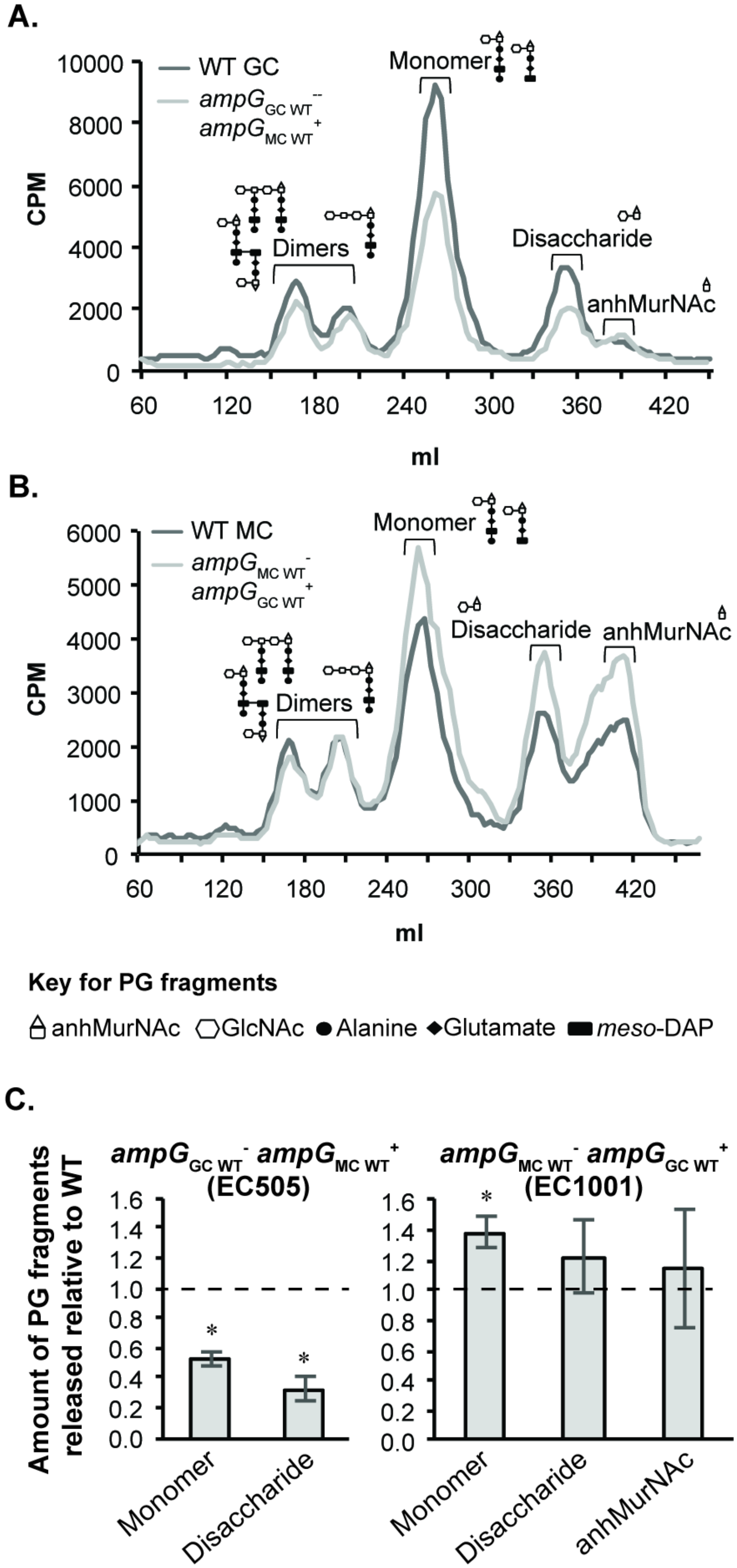
A.
WT GC
ampGGC WT-
ampGMC WT+
CPM
ml
Monomer
Dimers
Disaccharide
anhMurNAc
B.
WT MC
ampGMC WT-
ampGGC WT+
Key for PG fragments
anhMurNAc
GlcNAc
Alanine
Glutamate
meso-DAP
C.
Amount of PG fragments released relative to WT
ampGGC WT- ampGMC WT+ (EC505)
ampGMC WT- ampGGC WT+ (EC1001)
Monomer
Disaccharide
anhMurNAc

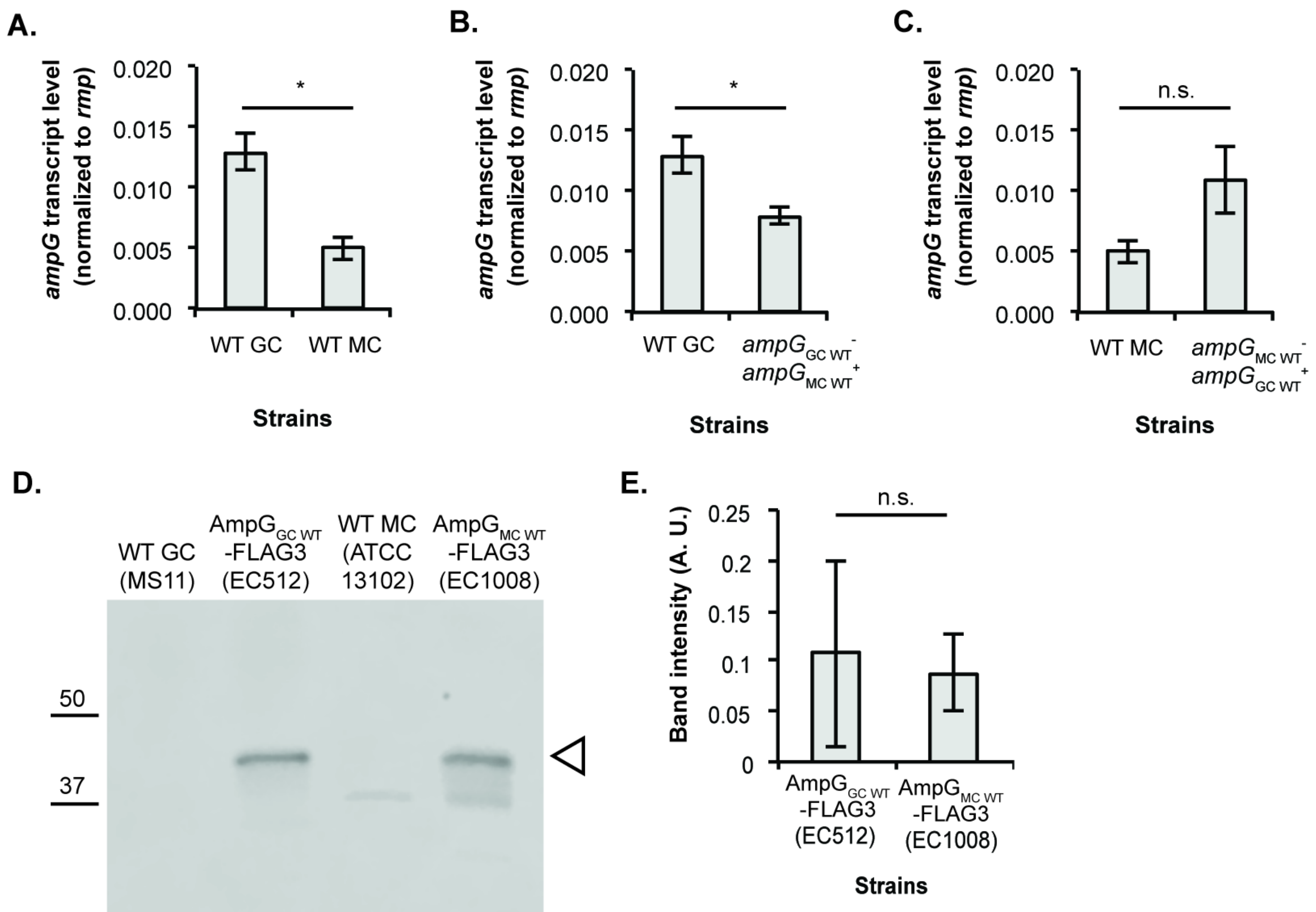
A.
B.
C.
ampG transcript level (normalized to rmp)
0.020
0.015
0.010
0.005
0.000
*
n.s.
WT GC
WT MC
ampG GC WT- ampG MC WT+
ampG MC WT- ampG GC WT+
Strains
D.
WT GC (MS11)
AmpG GC WT -FLAG3 (EC512)
WT MC (ATCC 13102)
AmpG MC WT -FLAG3 (EC1008)
50
37
E.
Band intensity (A. U.)
0.25
0.2
0.15
0.1
0.05
0
n.s.
AmpG GC WT -FLAG3 (EC512)
AmpG MC WT -FLAG3 (EC1008)
Strains

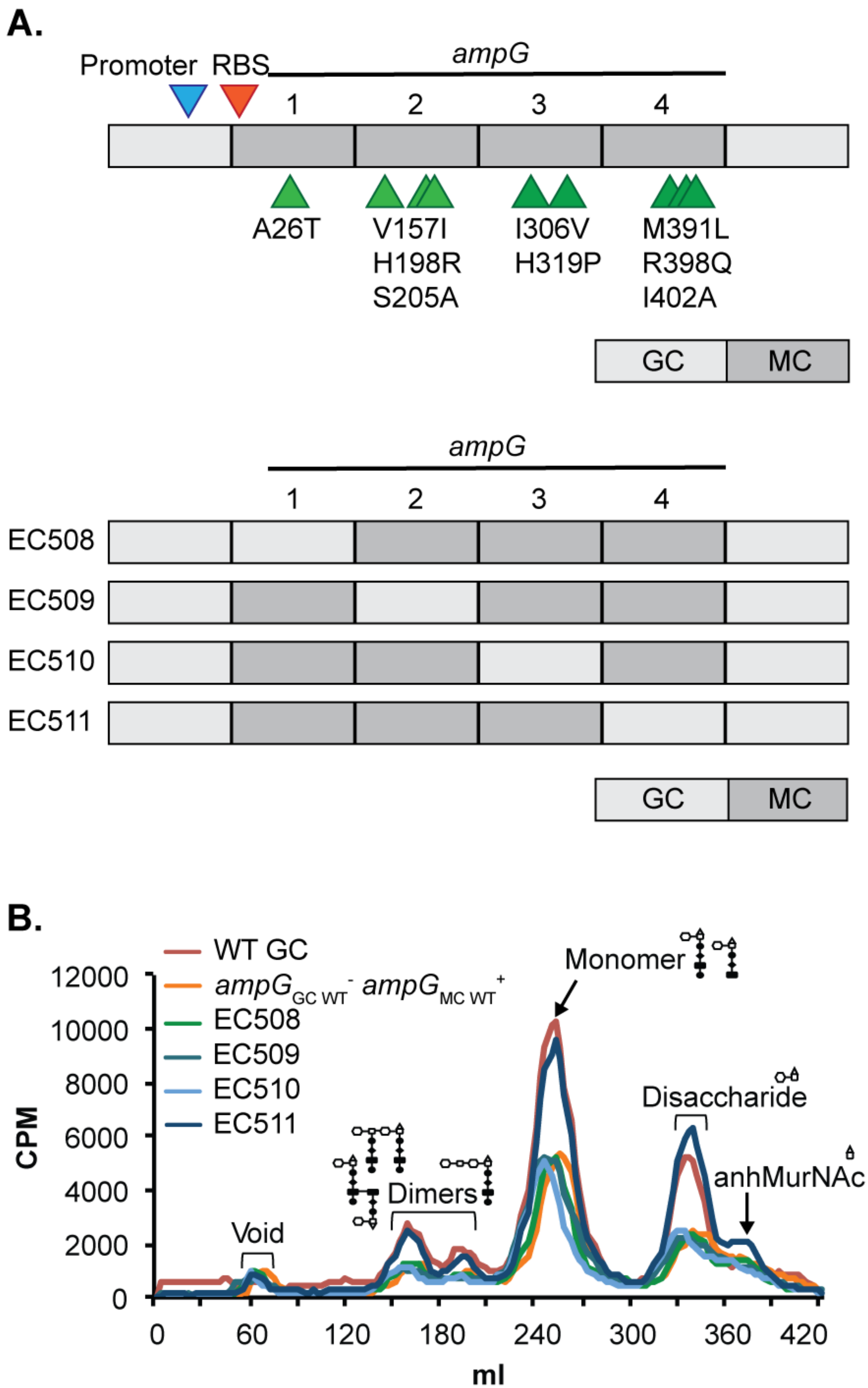

A.
Promoter
RBS
ampG
1
2
3
4
A26T
V157I
H198R
S205A
I306V
H319P
M391L
R398Q
I402A
GC
MC
ampG
1
2
3
4
EC508
EC509
EC510
EC511
GC
MC
B.
WT GC
ampG GC WT - ampG MC WT +
EC508
EC509
EC510
EC511
CPM
12000
10000
8000
6000
4000
2000
0
0
60
120
180
240
300
360
420
ml
Void
Dimers
Monomer
Disaccharide
anhMurNAc

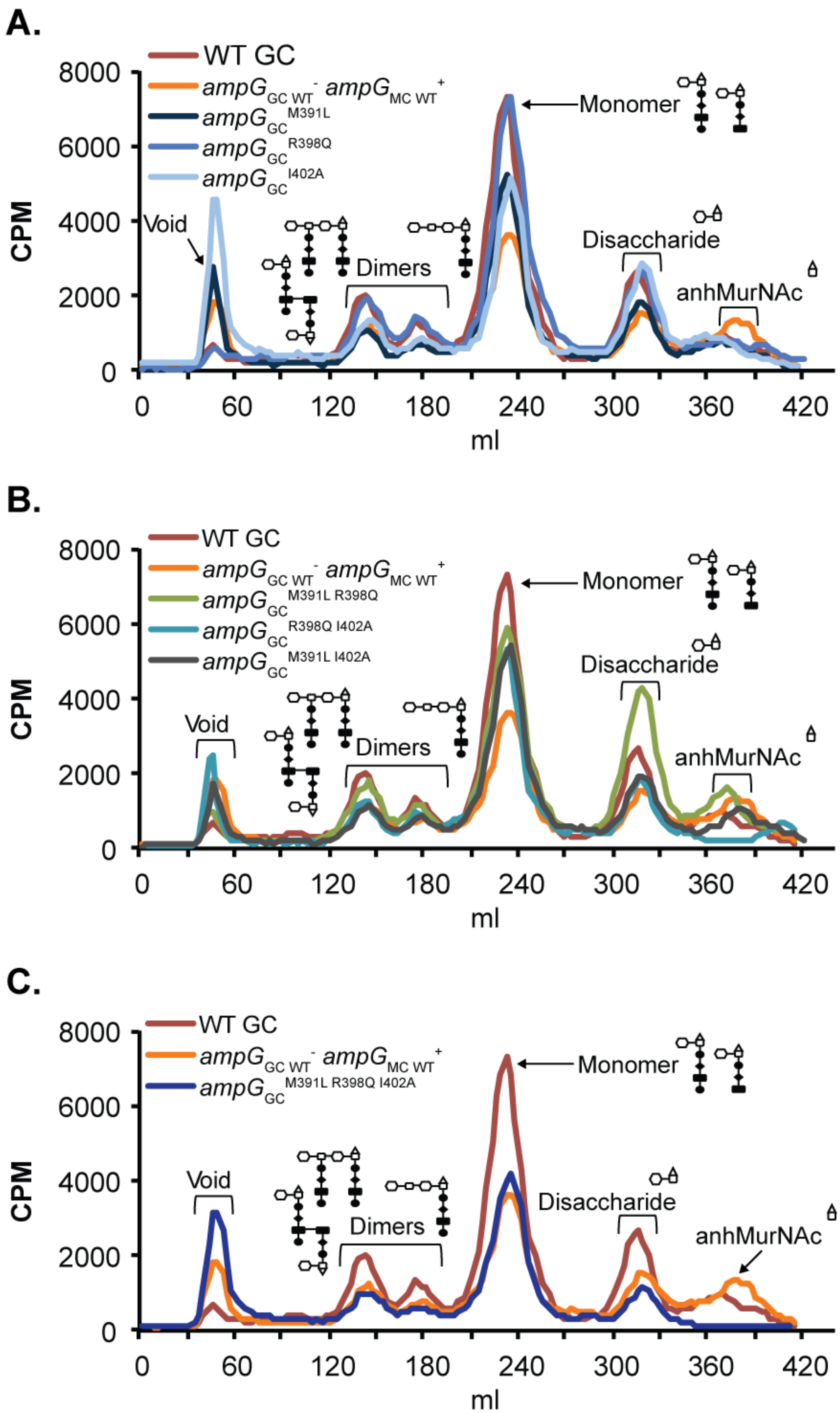
A.
WT GC
ampG GC WT - ampG MC WT +
ampG GC M391L
ampG GC R398Q
ampG GC I402A
CPM
ml
Void
Dimers
Monomer
Disaccharide
anhMurNAc
B.
WT GC
ampG GC WT - ampG MC WT +
ampG GC M391L R398Q
ampG GC R398Q I402A
ampG GC M391L I402A
C.
WT GC
ampG GC WT - ampG MC WT +
ampG GC M391L R398Q I402A

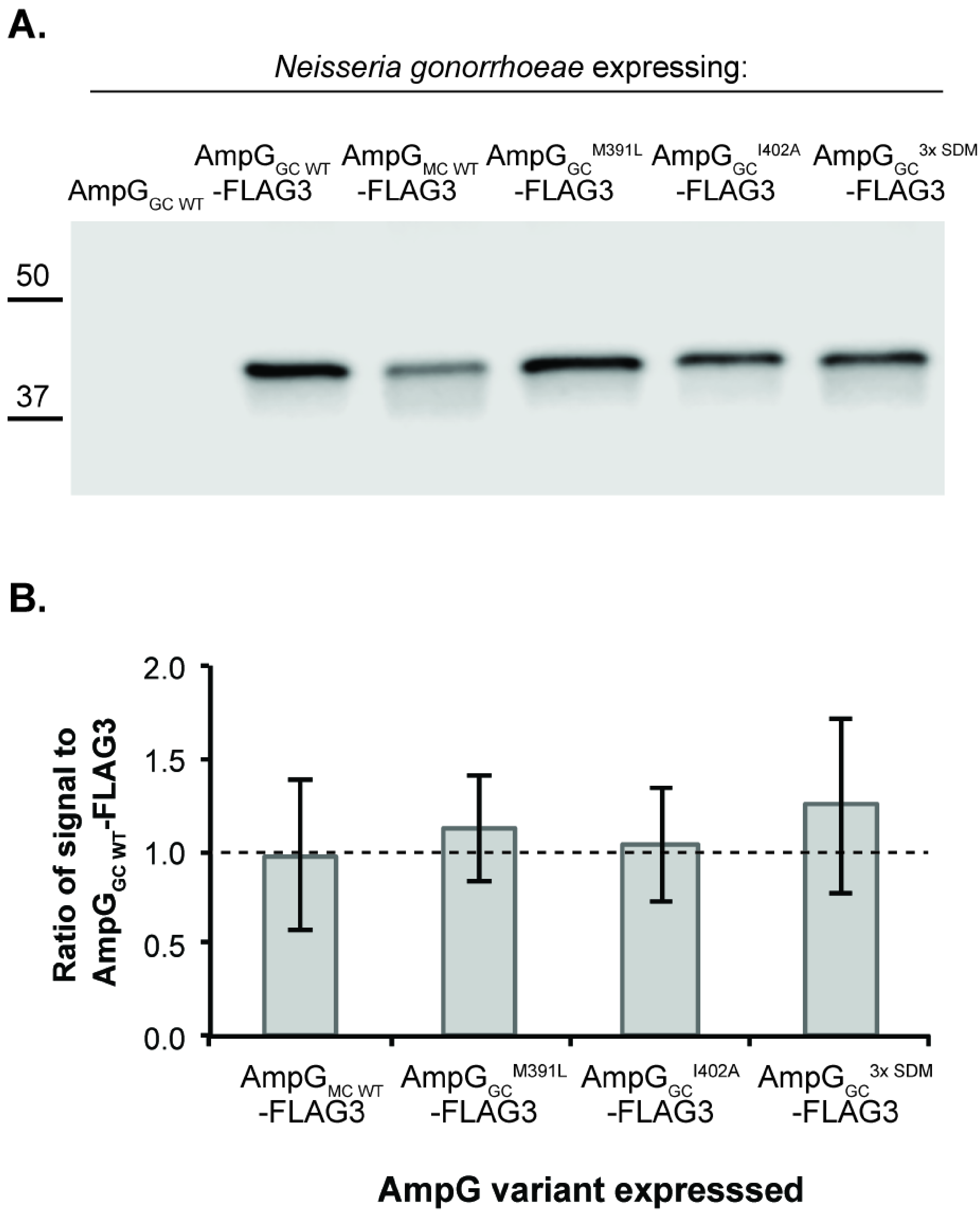
A.
Neisseria gonorrhoeae expressing:
AmpG GC WT
AmpG GC WT -FLAG3
AmpG MC WT -FLAG3
AmpG GC M391L -FLAG3
AmpG GC I402A -FLAG3
AmpG GC 3x SDM -FLAG3
50
37
B.
Ratio of signal to AmpG GC WT-FLAG3
2.0
1.5
1.0
0.5
0.0
AmpG MC WT -FLAG3
AmpG GC M391L -FLAG3
AmpG GC I402A -FLAG3
AmpG GC 3x SDM -FLAG3
AmpG variant expresssed

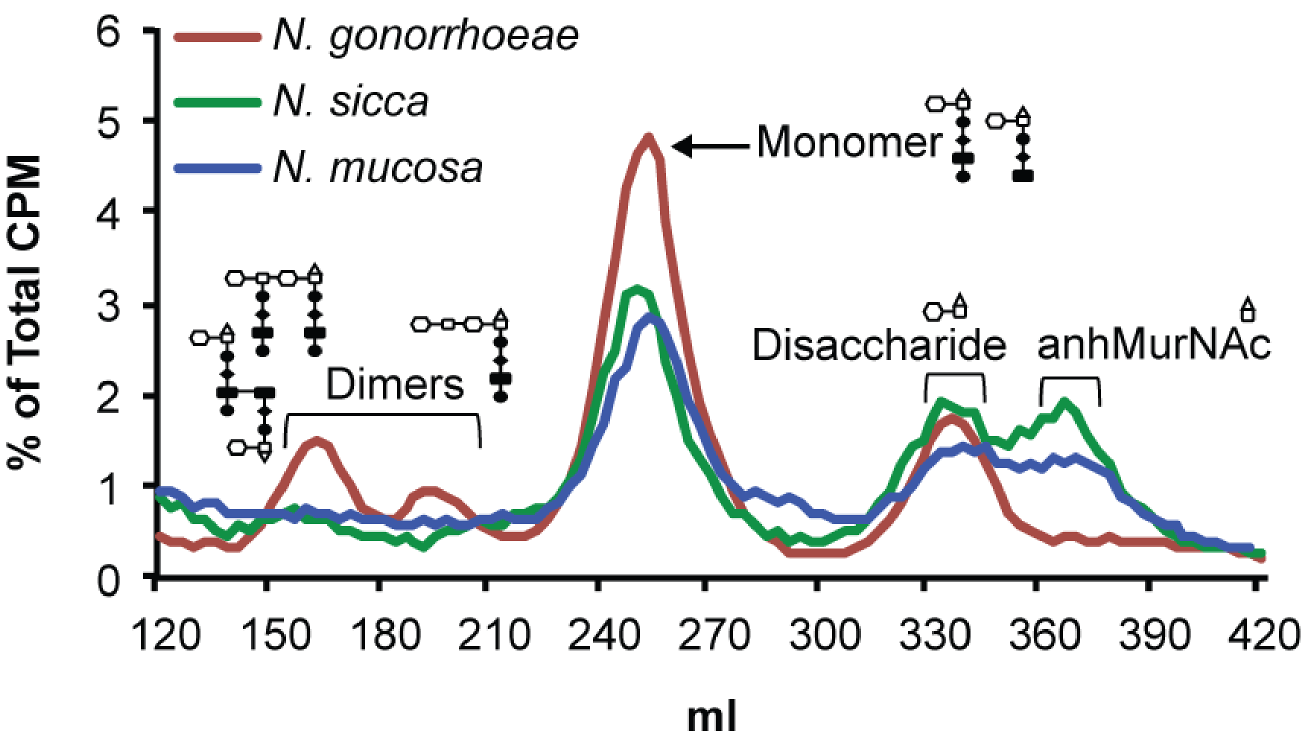
N. gonorrhoeae
N. sicca
N. mucosa
% of Total CPM
0
1
2
3
4
5
6
Monomer
Dimers
Disaccharide
anhMurNAc
120
150
180
210
240
270
300
330
360
390
420
ml

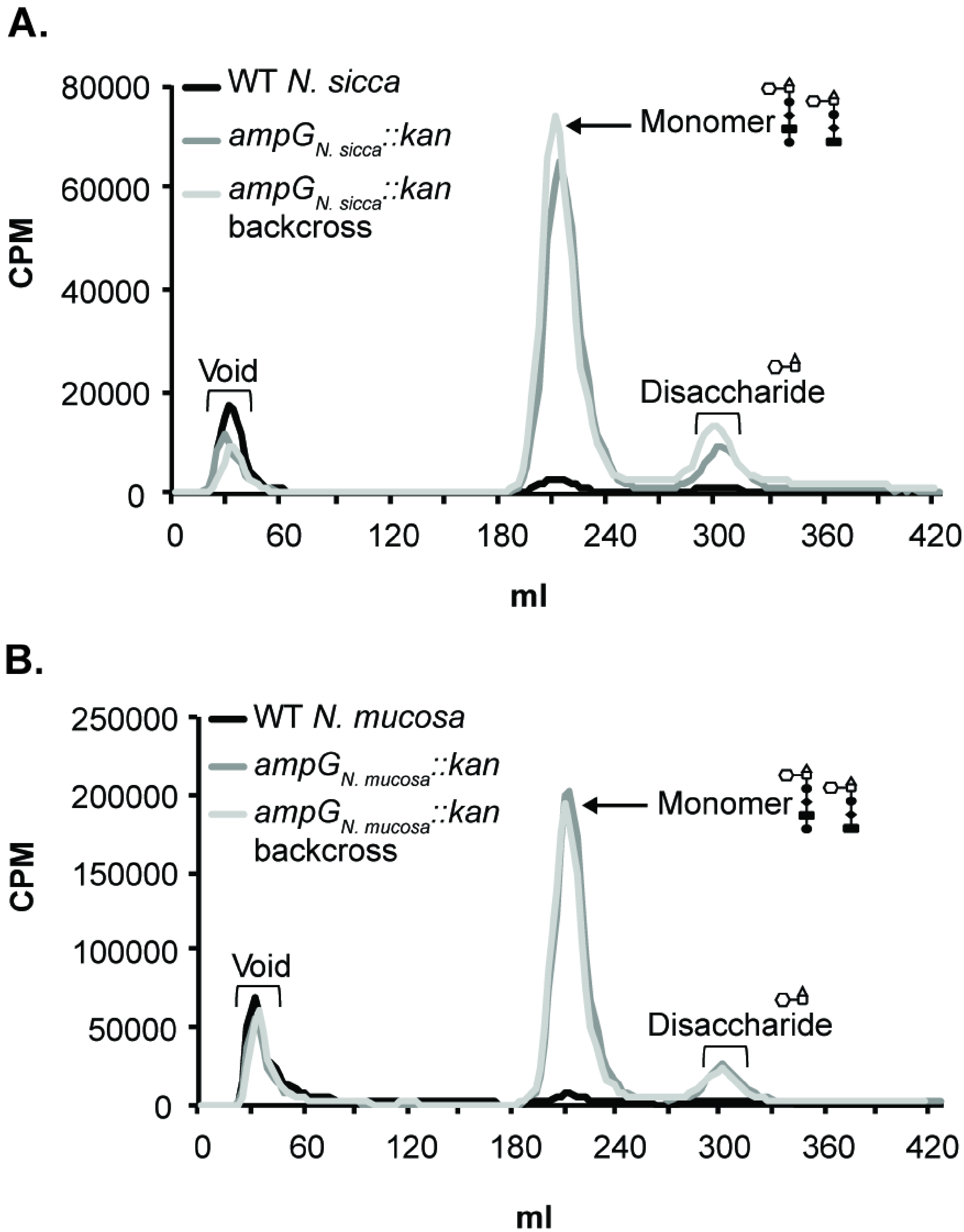
A.
80000
60000
40000
20000
0
CPM
WT N. sicca
ampG N. sicca ::kan
ampG N. sicca ::kan backcross
Monomer
Void
Disaccharide
0
60
120
180
240
300
360
420
ml
B.
250000
200000
150000
100000
50000
0
CPM
WT N. mucosa
ampG N. mucosa ::kan
ampG N. mucosa ::kan backcross
Monomer
Void
Disaccharide
0
60
120
180
240
300
360
420
ml

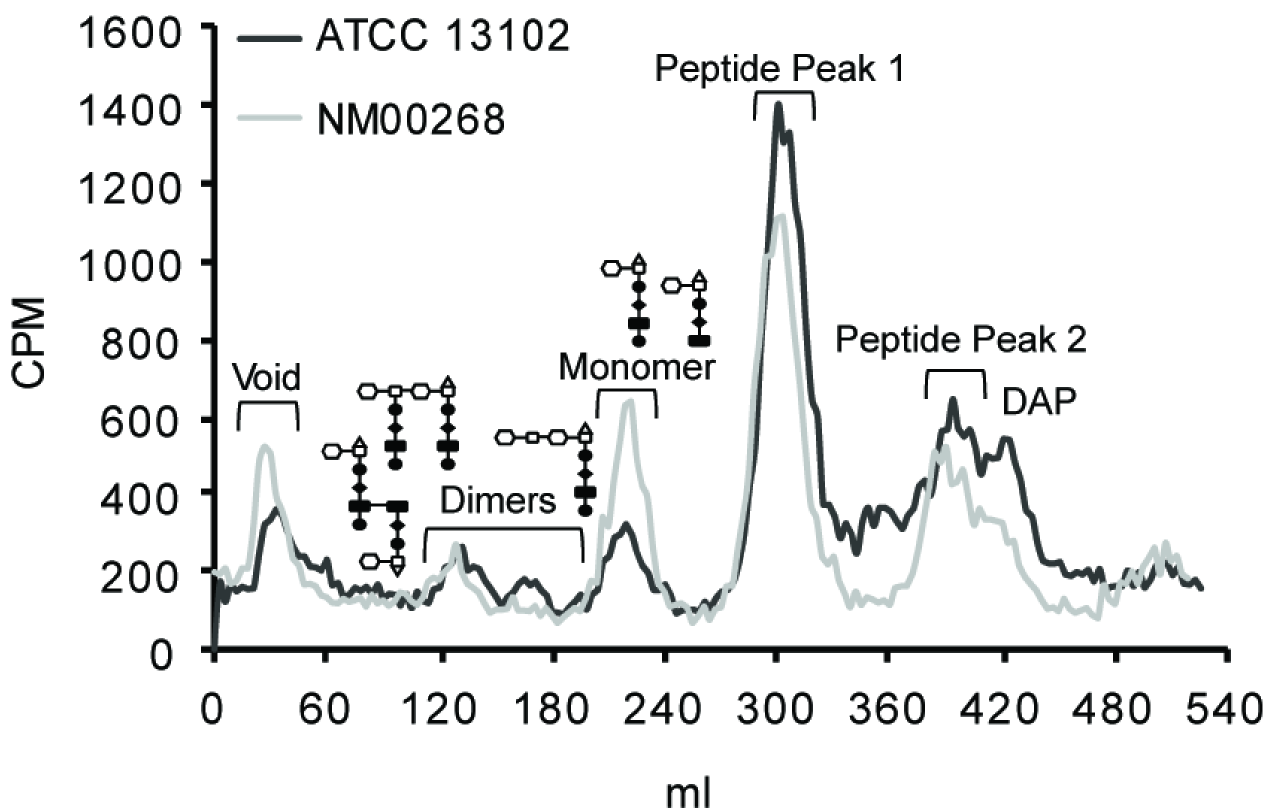

1600
1400
1200
1000
800
600
400
200
0
CPM
ATCC 13102
NM00268
Peptide Peak 1
Peptide Peak 2
DAP
Void
Dimers
Monomer
0
60
120
180
240
300
360
420
480
540
ml

A.

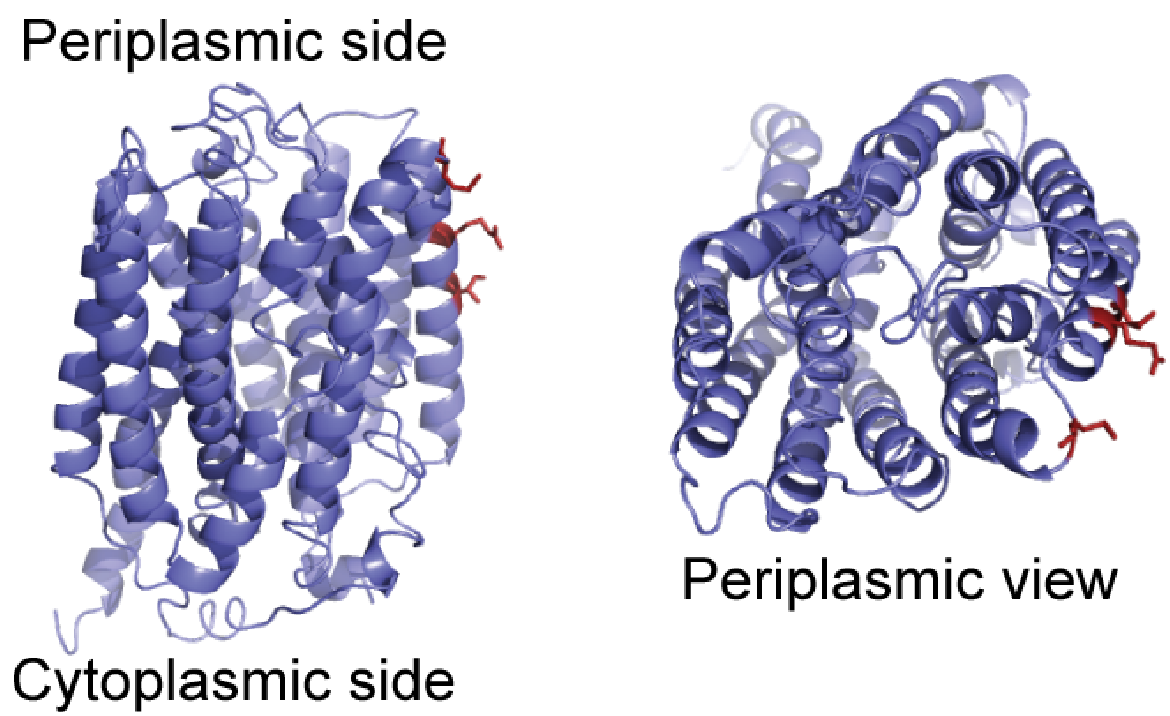
Periplasmic side
Cytoplasmic side
Periplasmic view

B.

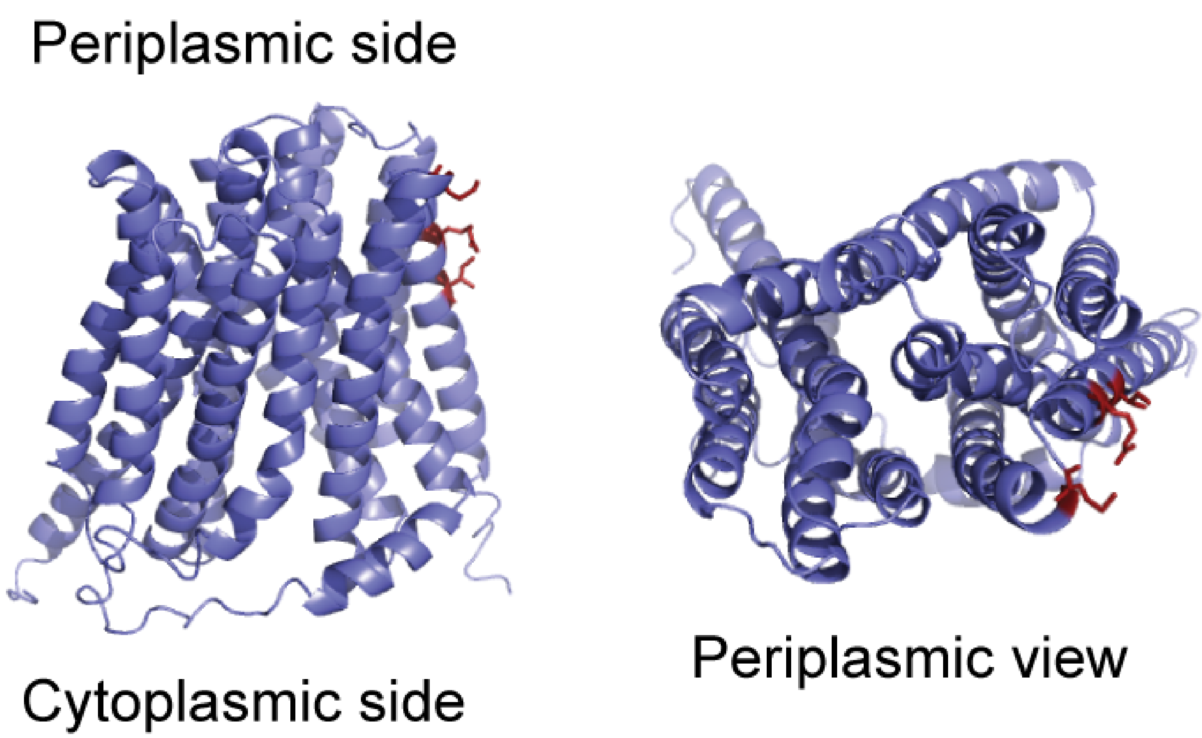
Periplasmic side
Cytoplasmic side
Periplasmic view